PUBLISHED VERSION

David McInerney, Mark Thyer, Dmitri Kavetski, Faith Githui, Thabo Thayalakumaran, Min Liu, George Kuczera

The importance of spatiotemporal variability in irrigation inputs for hydrological modelling of irrigated catchments

Water Resources Research, 2018; 54(9):6792-6821

© 2018. American Geophysical Union. All Rights Reserved.

DOI: http://dx.doi.org/10.1029/2017WR022049

PERMISSIONS

http://publications.agu.org/author-resource-center/usage-permissions/

Permission to Deposit an Article in an Institutional Repository

Adopted by Council 13 December 2009

AGU allows authors to deposit their journal articles if the version is the final published citable version of record, the AGU copyright statement is clearly visible on the posting, and the posting is made 6 months after official publication by the AGU.

15 November 2019

http://hdl.handle.net/2440/117626

AGU100 ADVANCING EARTH AND SPACE SCIENCE

Water Resources Research

RESEARCH ARTICLE
10.1029/2017WR022049

Key Points:
- The representation of spatiotemporal variability of irrigation inputs impacts substantially on distributed hydrological model simulations
- New stochastic irrigation schedule model developed to generate more realistic spatially variable event-based irrigation time series
- The new irrigation schedule model leads to improved catchment streamflow simulated using SWAT and enables uncertainty decomposition

Supporting Information:
- Supporting Information S1

Correspondence to:
D. McInerney,
David.Mcinerney@adelaide.edu.au

Citation:
McInerney, D., Thyer, M., Kavetski, D., Githui, F., Thayalakumaran, T., Liu, M., & Kuczera, G. (2018). The importance of spatiotemporal variability in irrigation inputs for hydrological modeling of irrigated catchments. *Water Resources Research*, *54*, 6792–6821. https://doi.org/10.1029/2017WR022049

Received 15 OCT 2017
Accepted 14 MAY 2018
Accepted article online 24 MAY 2018
Published online 23 SEP 2018

© 2018. American Geophysical Union. All Rights Reserved.

The Importance of Spatiotemporal Variability in Irrigation Inputs for Hydrological Modeling of Irrigated Catchments

David McInerney[1], Mark Thyer[1], Dmitri Kavetski[1,2], Faith Githui[3], Thabo Thayalakumaran[3], Min Liu[1], and George Kuczera[2]

[1]School of Civil, Environmental and Mining Engineering, University of Adelaide, Adelaide, SA, Australia, [2]School of Engineering, University of Newcastle, Callaghan, NSW, Australia, [3]Department of Economic Development, Jobs, Transport and Resources, Agriculture Research Division, Vic, Australia

Abstract Irrigation contributes substantially to the water balance and environmental condition of many agriculturally productive catchments. This study focuses on the representation of spatiotemporal variability of irrigation depths in irrigation schedule models. Irrigation variability arises due to differences in farmers' irrigation practices, yet its effects on distributed hydrological predictions used to inform management decisions are currently poorly understood. Using a case study of the Barr Creek catchment in the Murray Darling Basin, Australia, we systematically compare four irrigation schedule models, including uniform versus variable in space, and continuous-time versus event-based representations. We evaluate simulated irrigation at hydrological response unit and catchment scales, and demonstrate the impact of irrigation schedules on the simulations of streamflow, evapotranspiration, and potential recharge obtained using the Soil and Water Assessment Tool (SWAT). A new spatially variable event-based irrigation schedule model is developed. When used to provide irrigation inputs to SWAT, this new model: (i) reduces the over-estimation of actual evapotranspiration that occurs with spatially uniform continuous-time irrigation assumptions (biases reduced from ~40% to ~2%) and (ii) better reproduces the fast streamflow response to rainfall events compared to spatially uniform event-based irrigation assumptions (seasonally adjusted Nash-Sutcliffe Efficiency improves from 0.15 to 0.56). The stochastic nature of the new model allows representing irrigation schedule uncertainty, which improves the characterization of uncertainty in simulated catchment streamflow and can be used for uncertainty decomposition. More generally, this study highlights the importance of spatiotemporal variability of inputs to distributed hydrological models and the importance of using multivariate response data to test and refine environmental models.

Plain Language Summary In many regions irrigation is the primary water input for agriculture, and affects key productivity aspects such as the yield and quality of crops. From the hydrological perspective, irrigation affects important responses such as surface runoff, potential recharge, and actual evapotranspiration. Understanding and predicting these responses at relevant spatial and temporal scales is critical for efficient management of irrigated landscapes, in particular to improve agricultural productivity and ecosystem sustainability. This study evaluates irrigation schedule models that are used to provide inputs into spatially distributed hydrological models. We compare four of these models in terms of several criteria, including consistency with typical irrigation practices and ability to produce reliable hydrological simulations when fed as inputs into spatially distributed hydrological models. Our results emphasize the importance of representing spatiotemporal variability in irrigation inputs, with the best performance obtained using a new spatially variable event-based model. The findings provide guidance on the use of irrigation schedule models for hydrological modelling of irrigated catchments, as well as on the broader scientific question of representing variability in environmental processes.

1. Introduction

Irrigation contributes substantially to the water balance of many agriculturally productive areas. For example, in semiarid regions of Australia, irrigation water can represent more than a half of the inputs to the catchment water budget (e.g., Githui et al., 2012). Understanding the role of irrigation in the water balance of irrigated landscapes is hence of practical interest to modelers, decision-makers, and planners. Spatially distributed

hydrological models, such as the Soil and Water Assessment Tool (SWAT) (Arnold et al., 1998), which embody our current understanding of catchment behavior, can be used for this purpose. These models are increasingly used to inform management decisions (e.g., land use change) in irrigated catchments to optimize potentially competing objectives such as maximizing irrigation efficiency, the needs of groundwater dependent ecosystems (such as wetland/riparian zones) and managing salinity (Cau & Paniconi, 2007; Emam et al., 2015; Faramarzi et al., 2010; Githui et al., 2012; Maier & Dietrich, 2016; Sun & Ren, 2014).

One of the challenges in analyzing irrigation practices and their impact on the water cycle of irrigated catchments is the dearth of measured irrigation data. Given typical farmer irrigation practices, we expect irrigation depths to exhibit appreciable spatiotemporal variability. Temporal variability in irrigation arises due to the event-based nature of farm-scale irrigation. Spatial variability in irrigation arises due to differences in crop type, soil type, and farmer behavior across multiple farms. The timing of irrigation events may be based on the farmer's personal experience and visual observation of crops/soils (Montagu & Stirzaker, 2008), or, in some cases, on more "objective" methods such as monitoring soil water, evaporation and other environmental variables (Greenwood et al., 2009; Leib et al., 2002; Montagu & Stirzaker, 2008). Another major source of variability in irrigation depths is given by the constraints in the water delivery system and water costs.

"Irrigation schedule" models are often used to simulate the timing and depth of irrigation at various locations in a catchment, because irrigation data are seldom available at the small spatial scale required for inputs into distributed hydrological models such as SWAT. Irrigation schedule models can incorporate a range of information, including irrigation depths and intervals based on Best Management Practices (BMPs), planting dates recommended in technical reports of crop management (e.g., Cheema et al., 2014; Sun & Ren, 2013), meteorological conditions such as rainfall and actual evapotranspiration (AET) (Rahbeh et al., 2013), and local measurements of irrigation water use at larger spatial scales (e.g., at the scale of the entire catchment, Baubion et al., 2008; Chiew & McMahon, 1990; Githui et al., 2012). For example, BMPs for perennial pastures in Victoria, Australia, recommend irrigating when the difference between AET and precipitation is 50 mm, which typically occurs every 7 days in summer but less frequently during spring and autumn when actual evapotranspiration (AET) is lower (Greenwood et al., 2009; Lawson & Hildebrand, 2003).

This study evaluates how different spatiotemporal representations of irrigation inputs impact on the ability of a distributed hydrological model to simulate catchment responses such as streamflow, AET, and potential recharge.

There is a wide range of approaches for modeling irrigation schedules. In terms of *spatial variability in irrigation*, the following representations have been used:

1. Spatially uniform across land use types known to be irrigated (Baubion et al., 2008, Brauer & Gitz, 2012). This approach is simple to implement, but makes the unrealistic assumption that all farmers irrigate all crops on the same day across the entire catchment.
2. Spatial variability limited to different crop types. Examples of this approach include models that assume irrigation practices largely follow technical reports of crop water use (Cheema et al., 2014; Li et al., 2009), models based on crop types and observations of precipitation and AET (Rahbeh et al., 2013), and models that disaggregate measured catchment irrigation volume based solely on crop type and season (Githui et al., 2012). These approaches allow for spatial variability in irrigation schedules, but retain the unrealistic assumption that all areas with the same crop type will be irrigated on the same day.
3. Spatial variability represented at the discretization scale of the hydrological model, most often at the scale of hydrological response units (HRUs). Examples include models based on soil water/plant stress (e.g., Connell et al., 2001; Neitsch et al., 2011) and models that disaggregate catchment irrigation volume to the HRU scale (Githui et al., 2016). HRU scale irrigation schedule models can exhibit more spatial variability than models based solely on crop type—at the expense of increased model complexity (including additional assumptions) and/or additional data requirements.

In terms of *temporal variability in irrigation*, the following representations can be distinguished:

1. Continuous in time, e.g., individual HRUs are assumed to be irrigated every day with no breaks. This approach is typically used in conjunction with the spatially uniform approach, e.g., in cases where catchment irrigation is known or estimated over a period of time (Baubion et al., 2008; Chiew & McMahon, 1990; Marillier et al., 2009), or when annual crop irrigation can be estimated (Brauer & Gitz, 2012);

2. Event-based irrigation approaches, which better reflect the patterns in the farmers' irrigation practices in terms of irrigation intervals and depths (e.g., Connell et al., 2001; Neitsch et al., 2011). Event-based approaches require their own set of modeling choices and assumptions in order to simulate the timing and depths of irrigation events (e.g., Githui et al., 2016).

The wide range of approaches used in irrigation schedule modeling leads to the first research question: *From a pragmatic perspective, how "realistic" should spatial and temporal irrigation inputs be in order to achieve hydrological model simulations fit for the purpose of supporting environmental management decisions*? While some publications have studied irrigation inputs and their impact on hydrological model simulations (e.g., Githui et al., 2016; Kannan et al., 2011), we are not aware of studies that have systematically compared multiple representations of spatiotemporal variability in irrigation. It is common in environmental modeling to neglect spatiotemporal variability even in major hydrological forcings. For example, in one-dimensional (lumped) rainfall-runoff modeling, it is often assumed that the inputs (rainfall and potential evapotranspiration) and states (storage) are spatially uniform over entire catchments. Despite these assumptions, it is generally accepted that these models provide simulations of sufficient quality for many research and forecasting applications (e.g., Bergström, 1995; Perrin et al., 2003; Tuteja et al., 2012). Can spatiotemporal variability be ignored in irrigation schedule modeling?

Representations of spatiotemporal variability are inherently linked to the spatiotemporal discretization used in the hydrological model and its inputs. A highly refined discretization is inherently capable of capturing finer process variations than a coarse discretization, yet such refinement is inevitably limited by data availability and computational cost (e.g., Beven & Pappenberger, 2003; Clark et al., 2011). Once the spatiotemporal scales of a hydrological model and its inputs are specified, subscale variability is often ignored. The inability of a model to capture the subscale spatiotemporal variability of an environmental process manifests itself as simulation uncertainty and can be represented using stochastic models (e.g., Kandel et al., 2005; Renard et al., 2011).

In many applications, including this study, the spatial sampling scale of observed irrigation inputs (catchment scale) is much coarser than the spatial discretization of the hydrological model (HRU scale). The distinct irrigation schedule model approaches listed above relate to different representations of subsampling-scale variability in irrigation, to disaggregate from the sampling scale to the model scale.

This leads to the second research question: *Given that the spatiotemporal distribution of irrigation is highly uncertain (due to the absence of high resolution measurements) how important is it to represent irrigation schedule uncertainty in irrigation inputs*? It is unclear how large the uncertainty in simple irrigation schedule models is, how this uncertainty propagates through the hydrological model, and how it impacts on hydrological simulations.

In pursuit of these research questions, this study has the following aims:

1. Introduce a new stochastic irrigation schedule model that produces spatially variable event-based irrigation schedules and allows quantification of uncertainty in the simulated irrigation.
2. Compare the new irrigation schedule model against multiple existing representations. Evaluate the impact of different representations of spatiotemporal variability in irrigation on the simulations of streamflow, actual evapotranspiration, and potential recharge obtained using a distributed hydrological model. This analysis is undertaken at the HRU and catchment scales.
3. Use the new irrigation schedule model to evaluate the contribution of uncertainty in irrigation schedules on the uncertainty in hydrological simulations.

The remainder of the paper is organized as follows. Section 2 introduces the irrigation schedule models used to investigate spatiotemporal variability, and presents a new spatially variable event-based model where uncertainty in irrigation schedules is represented stochastically. The next three sections describe the case study: section 3 describes the case study area and hydrological model setup, section 4 describes the calibration of the hydrological model and the estimation of simulation uncertainty, and section 5 describes the methods used to evaluate these simulations. Section 6 presents the case study results. Section 7 discusses the influence of representations of spatiotemporal variability in irrigation inputs on the simulation of irrigation and hydrological variables. Section 8 summarizes the key conclusions.

2. Representations of Spatiotemporal Variability in Irrigation Schedule Models

2.1. Basic Definitions

A hydrological model H simulates hydrological processes as a function of forcing data $\mathbf{X}$, hydrological model parameters $\boldsymbol{\theta}_H$, and initial conditions $\mathbf{S}_0$,

$$\hat{\mathbf{Y}} = H(\mathbf{X}; \boldsymbol{\theta}_H, \mathbf{S}_0) \tag{1}$$

The simulated responses $\hat{\mathbf{Y}}$ provide an approximation to observed data $\tilde{\mathbf{Y}}$, and may include time series of streamflow at given locations, AET over specified areas, and so forth. The forcing data $\mathbf{X}=\{\mathbf{X}_C, \mathbf{X}_I\}$ comprise climate inputs $\mathbf{X}_C$, such as rainfall and temperature, and irrigation inputs $\mathbf{X}_I$, such as the depth and timing of irrigation.

Irrigation inputs at the model scale are typically not observed, and are hence estimated using an irrigation schedule model I. In this study, we consider irrigation schedule models that disaggregate the observed catchment irrigation volume $\mathbf{D}_I$, provided as an input to the model, according to an assumed representation of spatiotemporal variability,

$$\mathbf{X}_I = I(\mathbf{D}_I; \boldsymbol{\theta}_I) \tag{2}$$

where $\boldsymbol{\theta}_I$ are the irrigation model parameters.

2.2. Existing Irrigation Schedule Models

Three existing irrigation schedule models are included, in order to motivate the development of the new spatially variable event-based irrigation schedule model (Aim 1), and to provide multiple representations of spatiotemporal variability as part of irrigation schedule model analyses (Aim 2).

The selection of the existing irrigation schedule models follows the method of multiple hypotheses (see Clark et al., 2011). All models receive similar input data and their structures differ in a controlled way; differences in model performance can hence be attributed to differences in the model representation of spatiotemporal variability in irrigation. The shared input data comprises:

1. daily time series of observed catchment irrigation volume, which is estimated from the water supply system (see section 3.2);
2. irrigation season dates for specific crop types;
3. areas of individual HRUs; and
4. nominal irrigation depth for each crop type (only for event-based models), which is the amount of water applied in a single irrigation event. This parameter may be informed by Best Management Practices (BMPs) in the irrigation region; e.g., in Northern Victoria, Australia, irrigation volumes of ~50 mm per event are recommended (see section 3.2).

We consider multiple representations of spatial variability (uniform and variable) and temporal variability (continuous and event-based), yielding the three classes of irrigation schedule models listed next. Figure 1 provides an overview of the key steps for each irrigation schedule model, Figure 2 shows representative time series, and Appendix A provides complete algorithmic details.

Spatially Uniform, Continuous-Time (SU-C). The simplest approach to disaggregating observed daily catchment irrigation to the HRU scale is to apply it uniformly over all irrigated HRUs (Appendix A1). This approach ignores spatial variability and effectively ignores temporal variability: simulated irrigation varies in time solely due to daily variations in observed catchment irrigation, rather than due to discrete irrigation events at HRU scales. This representation results in unrealistically small irrigation depths every day, as seen in Figure 2a, and is not commonly used in the literature. It is included in this study in order to evaluate the impacts of introducing different representations of spatial and temporal variability, while still matching the observed catchment scale irrigation.

Spatially Uniform, Event-Based (SU-EB). This approach recognizes the event-based nature of irrigation at the farm-scale (Githui et al., 2012). The observed daily catchment irrigation is still disaggregated uniformly to the HRU scale, but unlike the SU-C model, this irrigation water is not applied immediately to the HRU on that day. Instead, the model accumulates this irrigation water over the "irrigation interval," defined as the period over which the "nominal" irrigation depth is reached. The HRU irrigation event is assumed to take place at the end of the irrigation interval (see Figure 1 and Appendix A2). This model simulates spatially uniform irrigation (similar to SU-C): on a given day, the same irrigation depth is applied over all irrigated HRUs of a given crop type—see Figure 2b for representative time series.

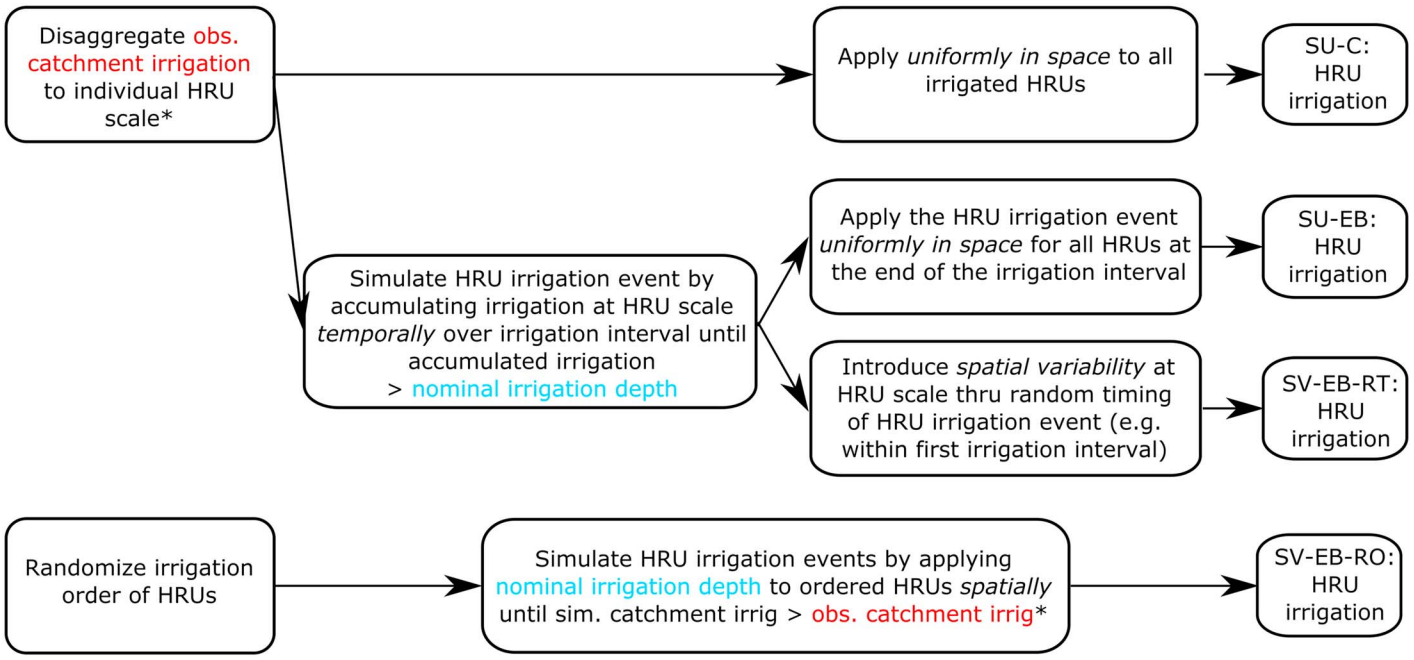

Figure 1. Flow chart of key steps of the irrigation schedule models considered in this work. The key inputs, namely the observed catchment irrigation and the nominal irrigation depth, are highlighted in blue and red fonts respectively. Other inputs, namely the HRU areas and the irrigation season dates for specific crop types, are used in the steps denoted by an asterisk (*).

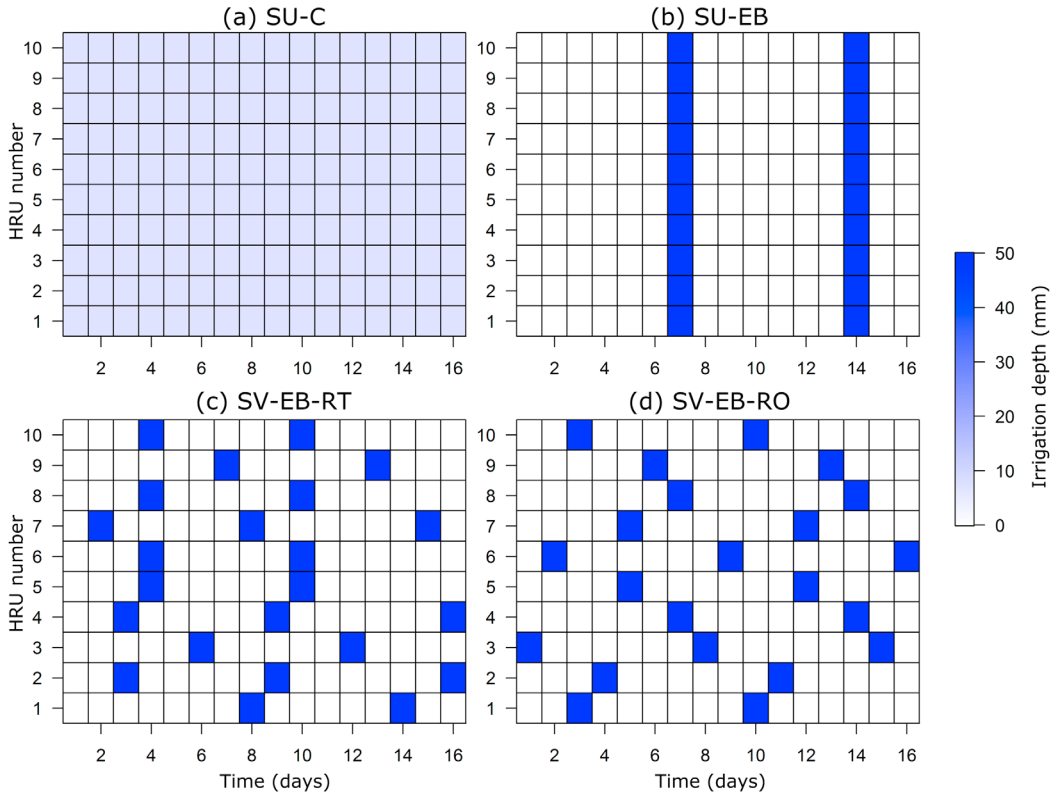

Figure 2. Representative time series of HRU scale irrigation simulated by the irrigation schedule models. Irrigation depths are shown over a period of 16 days, over a hypothetical area comprising 10 individual HRUs with same crop type.

Spatially Variable, Event-Based Approaches (SV-EB). Two instances of such irrigation schedule models are considered: an existing model from Githui et al. (2016) and the new model proposed in this study (section 2.3).

SV-EB Based on Random Irrigation Timing (SV-EB-RT). Githui et al. (2016) introduced spatial variability by modifying their earlier SU-EB model (Githui et al., 2012) so that the HRU irrigation event takes place at a random day during the first irrigation interval rather than at the end of it (see Figure 1 and Appendix A3, which also lists a minor modification in our implementation). The random timing of discrete irrigation events across multiple HRUs results in spatially variable event-based (SV-EB) irrigation—hence the model is named SV-EB-RT ("RT" denotes "random timing"). Figure 2c displays representative time series from this model. The uncertainty in irrigation depths can be represented stochastically, using multiple replicates of simulated irrigation generated by randomly varying the timing of the irrigation release within the first irrigation interval. Note that the replicates will differ in the timing of irrigation events even if the underlying irrigation intervals are identical. Note also that, due to the random timing of irrigation, the daily catchment irrigation simulated by the SV-EV-RT model does not always match the observed daily catchment irrigation, even if longer-term volumes are matched.

2.3. New Spatially Variable Event-Based Irrigation Schedule Model

We introduce a new spatially variable event-based irrigation schedule model, namely an *SV-EB model based on random irrigation order (SV-EB-RO)*. The SV-EB-RO model is motivated by the SV-EB-RT model of Githui et al. (2016), but is designed to address the mismatch between observed and simulated catchment irrigation at the daily scale. The new SV-EB model randomizes the *order* of irrigation rather than the *timing* of irrigation—hence it is named *SV-EB-RO* where "RO" denotes "random order." As part of algorithm initialization, the order in which HRUs will be irrigated over the irrigation season is selected randomly (this order is then kept fixed over the irrigation season). On the first day of the irrigation season, the daily observed catchment irrigation is used to irrigate as many HRUs as possible to their nominal irrigation depth, starting with the first HRU in the irrigation order and so on, until the simulated catchment irrigation volume reaches the observed catchment irrigation volume on that day. This procedure is repeated for all remaining days in the irrigation season, cycling through the HRUs according to the irrigation order. By construction, this procedure constrains the simulated catchment irrigation to be similar to the observed irrigation volume, with minor discrepancies due to daily carryover of small amounts of remaining irrigation water that is insufficient to fully irrigate the next HRU (Appendix A3).

Figure 1 illustrates that the SV-EB-RT model results from a minor modification to the SU-EB model, by randomizing the irrigation event date within the irrigation interval. In contrast, the SV-EB-RO model uses a very different approach to disaggregating the observed daily catchment irrigation, in which explicit constraints are applied to the simulated daily catchment irrigation.

The SV-EB-RO algorithm is stochastic: the uncertainty in the simulated spatiotemporal distribution of irrigation is represented using multiple replicates that differ in the HRU irrigation order, which is randomized at the start of the algorithm; Figure 2d displays representative irrigation time series.

It is worth noting that a (deterministic) irrigation time series from the SU-C model corresponds to average irrigation generated using the SV-EB-RO model with an infinite number of replicates.

2.4. Alternative Approaches to Irrigation Schedule Modeling

An alternative type of irrigation schedule models is given by models driven by the hydrological model states. These models tend to be embedded in the hydrological model itself, and typically assume that irrigation events occur when simulated water stress or total soil water in the profile crosses a threshold value. This type of irrigation schedule model is referred to as "autoirrigation" in SWAT (e.g., see Neitsch et al., 2011 for description, and Faramarzi et al., 2009; Zeng & Cai, 2014, for examples). This approach contrasts with the irrigation schedule models used in this study, which generate irrigation schedules prior to the hydrological model run and hence fall into the category of "manual irrigation" as defined in the SWAT user guide (Neitsch et al., 2011).

Autoirrigation approaches have the following limitations:

Despite wide usage, a number of studies have found that the SWAT autoirrigation model is often unable to reproduce expected irrigation practices (e.g., Chen et al., 2018; Githui et al., 2016; Kannan et al., 2011). For example, Githui et al. (2016) reported that this irrigation schedule model did not capture the seasonal irrigation patterns in the Toolamba catchment in South Eastern Australia, while Kannan et al. (2011) found that the depths, frequency and timing of simulated irrigation in an application to the Arroyo Colorado watershed in

Texas, USA, were unrealistic compared with expected farmer behavior. To explain the poor performance of the SWAT autoirrigation model, Chen et al. (2018) highlight some practical issues of this model, including the simulation of irrigation for crops even after they have been harvested. Note that Connell et al. (2001) presented an approach similar to autoirrigation that depends on the hydrological model states and is able to capture observed catchment irrigation at the *monthly* scale, but that study did not evaluate the simulated irrigation at the *daily* scale;

A general limitation of autoirrigation approaches is the assumption that daily irrigation occurs whenever the soil/plant needs it. This assumption is unrealistic—in practice, daily irrigation schedules vary from farmer to farmer and may be constrained by farm water delivery systems and water restrictions. The irrigation schedule models used in this study incorporate these constraints implicitly by using the observed daily catchment irrigation as an input.

For these reasons, the SWAT autoirrigation model is not used in this study.

3. Case Study Description

3.1. Study Area

The Barr Creek catchment is part of the Murray Darling Basin in Northern Victoria, Australia, and has an area of approximately 60,000 ha (Figure 3). The climate is semiarid, with hot summers, and annual rainfall varies from approximately 100 mm in dry years to 700 mm in wet years. The catchment is characterized by flat topography, deep drains, a shallow aquifer (Shepparton Formation), and a deeper aquifer (Deep Lead aquifer) that represents a deep regional groundwater system. The major soil types in the catchment are classified as medium clay (59%), heavy clay (24%), and light sand (17%) by Githui et al. (2012). The dominant land cover is pasture (predominantly annual and perennial). In 2002/2003 (the period considered in the case study), approximately 60% of the catchment was irrigated, with irrigation water making up more than 50% of the inputs to the annual water budget (~325 mm compared with ~285 mm of rainfall) (Githui et al., 2012). AET is the dominant component of outputs to the water budget, accounting for ~70%.

Irrigation water use varies throughout the irrigation season (between August and May) depending on crop water requirements and irrigation water availability; it is typically highest in summer when potential evapotranspiration (PET) is largest. Perennial pasture is irrigated throughout the irrigation season, while annual pasture is not irrigated in summer. Flood irrigation is the dominant irrigation method. In some farms, reuse dams are used to collect excess irrigation runoff from the paddocks to recycle the irrigation water, however the recycled volume is considered to be relatively minor (Sinclair Knight Merz, 2005). Excess irrigation water is removed through artificial drains that intersect the water table, allowing groundwater to discharge into the drains (Connell et al., 2001). During the study period, very little groundwater discharged into the drains due to the water table being low. Further details of the study area can be found in Githui et al. (2012).

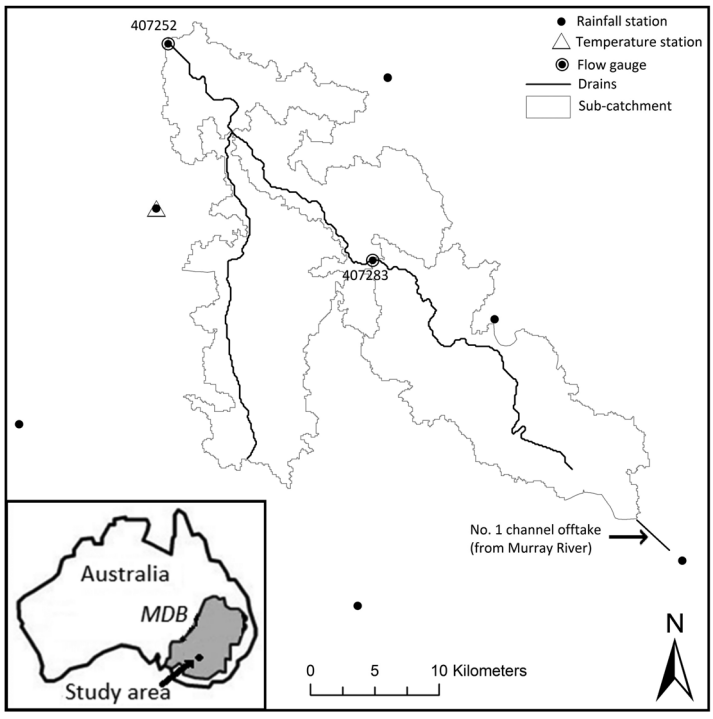

Figure 3. Barr Creek catchment study area (35.6°S–36.0°S, 143.9°E–144.4°E). Inset: map showing location of study area in the Murray Darling Basin (MDB) in Australia.

3.2. Data

3.2.1. Input Data for the Irrigation Schedule Models

Observed catchment irrigation was obtained by Selle et al. (2010) from the measured annual water supply into the Barr Creek catchment and the daily water delivered through the No. 1 Channel (see Figure 3). Selle et al. (2010) found that the measured annual water supply into the Barr Creek catchment was strongly correlated with the annual water supply through the channel offtake, with water delivered through the channel accounting for 60% of the total irrigation water use in the catchment (with the remaining 40% supplied through other channels). This correlation was used to estimate daily catchment irrigation for the entire catchment from the daily data for

the No. 1 Channel. Note that we do not attempt to estimate the uncertainty in the catchment irrigation associated with this approximation, nor to account for the time it takes for the irrigation water to be transferred from the No. 1 Channel to the farms. These assumptions will be discussed in section 7.3.

The nominal irrigation depth for event-based irrigation is set to 50 mm, according to the assumption that Barr Creek farmers largely follow the BMPs for perennial pastures in Northern Victoria, Australia (Githui et al., 2012, 2016). In practice, irrigation depths are variable, due to crop and soil types and farmer practices. Our estimate of nominal irrigation depth is partially corroborated by the results of Connell et al. (2001), who used water order data to estimate the distribution of irrigation depths in the same catchment; their results suggest a median irrigation depth of around 60 mm (which is slightly higher than the BMPs), with 90% probability limits in the (approximate) range of 40–160 mm.

Irrigation season dates are taken from Githui et al. (2012). Typical farm size in this region is estimated to be approximately 400 ha, based on reported sizes of farms in Victoria in 2011 (Consortium Land, 2018).

3.2.2. Additional Information to Evaluate "Realism" of Irrigation Schedule Models

In this study, the realism of the irrigation schedules simulated by the models is evaluated using the following independent sources of information:

1. Irrigation intervals suggested by BMPs for the study region, which recommend irrigation to occur every 7 days in summer, and less frequently during spring and autumn (Greenwood et al., 2009; Lawson & Hildebrand, 2003).
2. Irrigation intervals suggested weekly by Irrigating Agriculture (2017) on the basis of measured and forecast AET and precipitation. In particular, for early December 2017, the recommended irrigation interval for Kerang in Northern Victoria, Australia, was 8 days, which is consistent with BMPs above.
3. Annual crop water requirements (combined rain and irrigation) for producing optimum yields for perennial pasture. These requirements have been estimated by Victorian Resources Online (2017) as ~1,300 mm per annum.

This information is used to evaluate the simulated irrigation intervals and total irrigation volume applied to individuals HRUs of the perennial pasture crop type which are irrigated in spring, summer and autumn. Note that more detailed local data on farmer water use in the study region, such as irrigation schedules on specific crops, is not available.

3.2.3. Input Data to Run the Hydrological Model

The hydrological model (SWAT, see section 3.3) requires rainfall, temperature, and soil data. Rainfall time series from seven gauge stations, as well as maximum and minimum temperatures from a single station, were obtained from the SILO patched point database (Githui et al., 2012). Soils data, grouped into light soils, medium and heavy clays, were obtained from Sargeant et al. (1978) and SKM (2007). Land use data derived from Landsat imagery taken over different seasons and grouped into eight classes were obtained from Spatial Sciences Group, Agriculture Victoria Research Division, Australia. Irrigation depths and application dates were obtained from the irrigation schedule model.

3.2.4. Data for Hydrological Model Calibration

The hydrological model was calibrated to daily streamflow and monthly AET data. Daily streamflow data were available from gauging stations at the catchment outlet and at an inner subcatchment (see Figure 3). Monthly AET was estimated from MODIS satellite imagery using the SEBAL algorithm (Githui et al., 2012) and aggregated to the subcatchment scale (Figure 3). AET estimates obtained using remotely sensed energy balance can have biases of up to 10–20% (Allen et al., 2011). These AET estimates will be referred to as "AET observations" in the remainder of this study, consistent with the usage of "streamflow observations." The period between January 2001 and July 2002 is used for model warmup. The period between August 2002 and June 2003 is used for model calibration and evaluation; the data from this period comprise time series of 288 days of streamflow observations (at both the catchment and subcatchment outlets), and time series of nine observations of monthly AET at each of the four subcatchments. In this case study, observations of potential recharge are not available.

3.3. Hydrological Model SWAT

This section summarizes the Soil and Water Assessment Tool (SWAT) (Arnold et al., 1998; Gassman et al., 2007), used in this work as the hydrological model that routes precipitation and irrigation into streamflow, AET, and potential recharge.

3.3.1. Basic Setup

In this study, SWAT is set to operate on a daily time step. The smallest spatial units that are modeled are the hydrological response units (HRUs), defined by the overlay of two spatial discretizations: (i) the delineation of a catchment into subcatchments connected by channels; and (ii) the grouping of areas with similar land cover, soil type and surface slope into "HRU types." An "HRU" is then defined as the portion of a subcatchment of a given HRU type. The HRU resolution is refined further as described in section 3.3.3, where we introduce the concept of HRU-splitting.

Spatially distributed inputs into SWAT include rainfall, irrigation, temperature, land cover, soil type, elevation, and land use management. Water balance is governed by changes in soil water content, precipitation, irrigation, surface runoff, AET, shallow groundwater exchanges, and potential recharge (water leaving the root zone that could potentially recharge the shallow and deep aquifers).

Surface water, which includes runoff from rainfall and irrigation, from individual HRUs is routed to the subcatchment outlet. Surface runoff due to rainfall is calculated using the SCS runoff curve number method. Surface runoff due to irrigation is calculated as an assumed constant fraction of irrigation (controlled by an irrigation runoff coefficient). Potential evapotranspiration is calculated in SWAT from air temperature using the Hargreaves method. A detailed description of the SWAT2009 version used in this study is given by Neitsch et al. (2011).

3.3.2. SWAT Model Configuration

The SWAT configuration used in this study is based on the earlier work by Githui et al. (2012). The delineation into subcatchments was based on a Digital Elevation Model (DEM), and the surface drain network was incised into the DEM and corrected using local measurement of depths. HRU types were assigned using the three soil types and eight land use types described in section 3.2.3. Extensive details on the data and methods used to develop the SWAT configuration can be found in Githui et al. (2012).

In this work, we discretize Barr Creek into four subcatchments and 24 HRU types. We consider two spatial configurations: a "large" HRU configuration with $4 \times 24 = 96$ HRUs and a "small" HRU configuration with 163 HRUs, where further discretization is performed to reduce size of certain HRUs (section 3.3.3).

3.3.3. Reducing HRU Size to Reduce Discretization Effects in Irrigation

The discretization of Barr Creek catchment into four subcatchments and 24 HRUs types results in some HRUs being much larger in area than others, in some cases greatly exceeding the typical farm size. For example, in this "large" HRU configuration, the largest HRU has an area of ~4,800 Ha, which is 12 times larger than the typical farm size of 400 Ha in the Barr Creek catchment (section 3.2). Such a coarse spatial discretization is problematic from the perspective of SV-EB models, because it is unlikely that an area corresponding to multiple farms would be irrigated in its entirety at the same time. This issue can result in large mismatch between observed and simulated catchment irrigation (see section 6.1.2).

To mitigate this deficiency, we developed a "small" HRU configuration with four subcatchments, where the large HRUs were split into multiple smaller HRUs while keeping the total number of HRU types fixed. The smaller HRUs have identical physical characteristics (e.g., land use type, soil type, and slope as given by the large HRU), but can receive different irrigation inputs. The small HRU configuration has HRU sizes closer to typical farm sizes, and is used to investigate the effect of spatial discretization on irrigation schedule modeling. Unless otherwise stated, results from the small HRUs are presented throughout this paper. Note that the naming convention of "large" and "small" HRU configurations is intended solely for the purposes of this paper and is not a reflection of HRU sizes in other SWAT studies. The implementation of the HRU-splitting approach in SWAT is described in section 3.3.4.

In practice, constraints on the irrigation supply system, as well as agricultural and/or economic reasons, may make it infeasible or undesirable for an entire farm to be irrigated on the same day. Therefore, while the small HRU configuration used in this study provides a better representation of the relevant spatial scales of irrigation than the large HRU configuration, it is likely still too coarse and likely to under-estimate spatial variability in irrigation. This potential limitation is discussed in section 7.3.

3.3.4. Modified Estimation of Time-of-Concentration Parameter

Section 3.3.3 described the motivation for splitting large HRUs into smaller HRUs more commensurate with typical farm sizes. In this work, SWAT is run both on the large HRUs (when using irrigation schedule models SU-C and SU-EB) and on small HRUs (when using the SV-EB-RO irrigation schedule model). To ensure consistency between the runs based on substantially different spatial discretization, we modified the SWAT model

code to calculate the time of concentration for each HRU as a function of subcatchment area (which was consistent between the small and large HRU configurations), rather than as a function of HRU area (which is reduced when an HRU is split). This modification is consistent with the approaches of Baumgart (2005), Ohio EPA (2008), and Smith Murphy (2010).

4. Hydrological Model Calibration and Uncertainty Estimation

4.1. Calibration of SWAT

SWAT is calibrated using the PEST software (Doherty, 2004), which implements the gradient-based Levenberg-Marquardt optimization algorithm and is widely used in the SWAT community (e.g., Githui et al., 2009; Govender & Everson, 2005; Wang & Melessa, 2005). A total of 38 SWAT parameters are calibrated, guided by the sensitivity analysis of Githui et al. (2012) (see Table 1).

The objective function used in the calibration is a weighted sum of squared residuals (Doherty, 2004),

$$\Phi(\boldsymbol{\theta}_H)=\sum_{k=1}^{N_y}\sum_{j=1}^{N_{j(k)}}\left[w_k\left(\hat{Y}_{k,j}(\mathbf{X};\boldsymbol{\theta}_H)-\tilde{Y}_{k,j}\right)\right]^2 \tag{3}$$

where $\tilde{Y}_{k,j}$ is the observed response and $\hat{Y}_{k,j}$ is the response simulated using SWAT with a given input $\mathbf{X}$ (which comprises rainfall, temperature, and irrigation inputs). The subscript k indexes the responses as follows: k=1 refers to catchment outlet streamflow, k=2 refers to subcatchment streamflow and k=3 refers to AET, giving a total of N_y = 3 responses. The subscript j indexes individual observed data points, and $N_{j(k)}$ is the total number of data points comprising response k. In this study, $N_{j(1)}$=$N_{j(2)}$=288 and $N_{j(3)}$=36, as described in section 3.2. The response weights w_k in equation (3) are assigned to be inversely proportional to the estimated standard deviation of the observations, i.e., $w_k \propto 1/\mathrm{sdev}[\tilde{Y}_{k,1:N_{j(k)}}]$, with values provided by Githui et al. (2012).

The objective function in equation (3) is minimized with respect to the SWAT parameters $\boldsymbol{\theta}_H$, yielding the optimal parameters $\boldsymbol{\theta}_H^{(opt)}$. The irrigation schedule model parameters $\boldsymbol{\theta}_I$, namely the nominal irrigation depth and crop irrigation seasons (see section 2.2), are fixed a priori (see section 3.2.1) and are not optimized as part of the hydrological model calibration.

Initial testing of the calibration procedure found that parameter estimates optimized using PEST depended substantially on the initial parameter estimates. This nonrobust behavior can be attributed to the limitations

Table 1
SWAT Parameters Calibrated in the Case Study

SWAT parameter name	Description	Assumed scale of variation	Units	Minimum	Maximum
ESCO	Soil evaporation compensation factor	Catchment		0.001	1
CN	Curve number	Soil/land use		35	99
SURLAG	Surface runoff lag coefficient	Catchment	days	0.01	10
ALPHA_BF	Base flow recession coefficient	Catchment	days	0.02	1
GWQMN	Threshold depth of water in the shallow aquifer required for return flow to occur	Catchment	mm	0.01	5,000
GW_REVAP	Groundwater revap coefficient	Catchment		0.02	2
REVAPMN	Threshold depth of water in the shallow aquifer for "revap" to occur	Catchment	mm	0.1	500
RCHRG_DP	Deep aquifer percolation fraction	Catchment		0.01	1
GW_DELAY	Groundwater delay	Catchment	days	0.001	30
SOL_AWC	Soil available water capacity	Soil		0.001	0.5
CRK	Crack volume potential of soil	Soil		0.01	0.9
IRR_SQ	Irrigation runoff coefficients, represented as a fraction of irrigation water applied	Month/crop		0.001	0.5

Note. A total of 38 parameters were calibrated. Some parameters are varied at the catchment scale (i.e., have the same value across all HRUs), some are varied by soil type (medium and heavy soils were grouped together into one class), CN is varied by combination of soil/land use types, and the irrigation runoff coefficients are varied on a monthly basis and by crop type. See Neitsch et al. (2011) and Githui et al. (2012) for further details.

of gradient-based optimization methods in dealing with discontinuities and other irregularities in the objective function, which in SWAT could arise due to internal thresholds and other nonlinearities (e.g., see Kavetski & Clark, 2010). In order to achieve more robust calibration results, we employ a simple multistart optimization approach (e.g., Kavetski et al., 2007; Skahill & Doherty, 2006), where multiple parameter sets are drawn randomly from predefined parameter ranges and used as initial estimates for PEST optimization. A total of 100 multistarts are used and the parameter set with the lowest objective function value is retained as the estimated global optimum.

Equation (3) can be used directly when SWAT is forced using a deterministic irrigation schedule model (e.g., SU-C or SU-EB). When SWAT is forced using a stochastic irrigation schedule model (e.g., SV-EB-RO), the calibration procedure is enhanced as described next.

4.2. Calibration of SWAT With Stochastic Irrigation Inputs

The stochastic nature of SV-EB models requires an enhancement of the calibration process to accommodate multiple replicates of irrigation inputs (and hence multiple replicates of SWAT simulations). The framework of equation (3) is augmented by averaging the SWAT responses over multiple irrigation schedule replicates (for a given SWAT parameter set $\boldsymbol{\theta}_H$),

$$\hat{Y}_{k,j}^{ave}(\boldsymbol{\theta}_H) = \frac{1}{N_{rep}^{irrig}} \sum_{r=1}^{N_{rep}^{irrig}} \hat{Y}_{k,j}(\mathbf{X}^{(r)}; \boldsymbol{\theta}_H) \tag{4}$$

where $\hat{Y}_{k,j}(\mathbf{X}^{(r)}; \boldsymbol{\theta}_H)$ is the rth replicate of the SWAT simulation of response k at data point index j, and N_{rep}^{irrig} is the total number of input replicates $\mathbf{X}^{(r)}$ pregenerated from the irrigation schedule model. The expected value of these simulations, $\hat{Y}_{k,j}^{ave}(\boldsymbol{\theta}_H)$, is then used in lieu of $\hat{Y}_{k,j}(\mathbf{X}; \boldsymbol{\theta}_H)$ in equation (3). Note that the averaging in equation (4) is performed on the SWAT responses given the individual irrigation replicates, rather than over the irrigation replicates themselves.

In this study, $N_{rep}^{irrig} = 10$. This relatively low number of irrigation time series replicates is dictated by the relatively lengthy SWAT model runtimes, especially in combination with the multistart optimization procedure (section 4.1). For example, when $N_{rep}^{irrig} = 10$, approximately 120 CPU days (using 2.6 GHz CPUs) were required to complete the multistart optimization, which was made feasible through the use of parallel computing. Note that alternative approaches for accounting for input uncertainty in calibration are available, but are expected to incur even higher computational costs, and are hence deferred to future work (section 7.2).

4.3. Uncertainty Estimation

4.3.1. Estimating Total Simulation Uncertainty in Streamflow and AET

Total simulation uncertainty in streamflow and AET is estimated using a postprocessing approach, where a statistical model is fitted a posteriori to the residual errors of the respective SWAT simulations. In this uncertainty estimation strategy, the SWAT parameters are kept fixed at the optimized values $\boldsymbol{\theta}_H^{(opt)}$ from the hydrological model calibration (section 4.1) rather than calibrated jointly with the parameters of the residual error model. The postprocessing approach to uncertainty estimation avoids problematic interactions between the parameters of the hydrological model and the parameters of the residual error model and is hence more operationally robust (Evin et al., 2014).

To reflect the heteroscedasticity of residual errors, i.e., larger errors in larger streamflows (and similarly for ET and recharge), log-transformations are used (McInerney et al., 2017),

$$\eta_{k,j} = \log\tilde{Y}_{k,j} - \log\hat{Y}_{k,j} \tag{5}$$

where $\eta_{k,j}$ is the jth residual of log-transformed response k. When using deterministic irrigation schedule models, $\hat{Y}_{k,j} = \hat{Y}_{k,j}(\mathbf{X}; \boldsymbol{\theta}^{(opt)})$, whereas when using stochastic irrigation schedule models, $\hat{Y}_{k,j} = \hat{Y}_{k,j}^{ave}(\boldsymbol{\theta}^{(opt)})$.

The residuals $\boldsymbol{\eta}$ are assumed to be Gaussian with zero mean and standard deviation σ_k,

$$\eta_{k,j} \sim N(0, \sigma_k) \tag{6}$$

The standard deviation of the residuals, σ_k, is estimated using the method of moments, i.e.

$$\sigma_k = \text{sdev}[\boldsymbol{\eta}_{k,1:N_{j(k)}}] \tag{7}$$

where sdev[**z**] denotes the empirical standard deviation of a sample **z**, and $\boldsymbol{\eta}$ is calculated using equation (5) after SWAT is calibrated.

The total simulation uncertainty is represented by the "total" simulation distribution $p(Y^{(\text{sim,total})})$, which reflects all sources of uncertainty accounted for in our case study. This distribution is constructed using the set of samples $(Y_{k,j}^{(\text{sim,total})(r)}, k=1..N_y, j=1..N_{j(k)}, r=1..N_{rep}^{resid})$, where N_{rep}^{resid} is the number of replicates, and the rth replicate is drawn as follows,

$$\eta_{k,j}^{(r)} \leftarrow N(0, \sigma_k) \tag{8}$$

$$Y_{k,j}^{(\text{sim,total})(r)} = \exp\left(\log \hat{Y}_{k,j} + \eta_{k,j}^{(r)}\right) \tag{9}$$

In equation (8), the symbol "←" denotes the process of sampling from a probability distribution.

4.3.2. Estimating Uncertainty in Streamflow and AET Due to Irrigation Schedule Uncertainty

The contribution of irrigation schedule uncertainty to the total simulation uncertainty in streamflow and AET is represented using the "partial" simulation distribution $p(Y_{k,j}^{(\text{sim,irrig})})$, which excludes residual error uncertainty. This distribution is constructed as the set of samples $(Y_{k,j}^{(\text{sim,irrig})(r)}, k=1..N_y, j=1..N_{j(k)}, r=1..N_{rep}^{irrig})$, where the rth sample is

$$Y_{k,j}^{(\text{sim,irrig})(r)} = \hat{Y}_{k,j}(\mathbf{X}^{(r)}; \boldsymbol{\theta}) \tag{10}$$

This approach represents a simple Monte Carlo propagation of irrigation schedule uncertainty.

5. Evaluation Methods and Performance Metrics

5.1. Irrigation Time Series

The simulated irrigation time series are assessed at the HRU and catchment scales. Although observed irrigation time series are not available at the HRU scale, subjective estimates of typical irrigation depths and intervals based on BMPs given in section 3.2 are used to evaluate these irrigation time series. For the SU-EB, SV-EB-RT, and SV-EB-RO models, the nominal irrigation depth is specified as an input; therefore, we evaluate the simulated irrigation inputs based on irrigation intervals. For SU-C irrigation, we assess both the irrigation depths and irrigation intervals. In addition, we evaluate the annual total amount of water (combined rain and irrigation) applied to individual HRUs with perennial crops irrigated from spring-to-autumn by comparing simulated annual totals against the estimated annual crop water requirements for perennial pasture described in section 3.2.2. Note that the modeling period of August 2002 to June 2003 (section 3.2.4) covers the entire irrigation season but not the entire year. Therefore, the annual total water amounts were calculated by adding irrigation over the modeling period to rainfall over the entire year.

At the catchment scale, we visually compare the simulated irrigation time series against observed catchment irrigation.

5.2. Hydrological Model Simulations

The hydrological responses simulated by SWAT are assessed at multiple scales as described below.

Daily Streamflow Simulations at the Catchment and Subcatchment Outlet. Streamflow accuracy is quantified using the Nash-Sutcliffe efficiency (NSE) (Nash & Sutcliffe, 1970), see equation (B1) in Appendix B. Given the strong seasonality of streamflow in the Barr Creek catchment, we also report a "seasonally adjusted" NSE_{SA} (Schaefli & Gupta, 2007, defined by equation (B2) in Appendix B.

Catchment Scale AET Simulations. The accuracy of catchment scale AET simulations is assessed at the monthly scale using the NSE and mean bias metrics (Appendix B).

HRU Scale AET Simulations. In the absence of observed HRU scale AET data, we limit our analysis of spatial variability in AET to a comparison of SWAT simulations forced by different irrigation schedule models, as described below.

First, we compare the amount and spatial variability of AET simulated by different irrigation schedule models. This variability is analyzed over the "total irrigable area of the catchment, defined as

$$A_j^{irrigable} = \sum_{h \in h\_irrigable(j)} A_h \tag{11}$$

where $h\_irrigable(j)$ denotes the set of irrigable HRUs on day j, i.e., the set of HRUs that could potentially be irrigated on day j. Note that $h\_irrigable(j)$ depends solely on the irrigation season dates for the HRU crop type (see sections 2.2 and 3.2.1) and does not depend on the irrigation schedule model.

The distribution of AET across the irrigable HRUs on a given day is summarized by the area-weighted proportion of irrigable HRUs with a given AET, $\omega_j^E(x)$, defined as follows:

$$\omega_j^E(x) = \frac{\sum_{h \in h\_E(x,j)} A_h}{A_j^{irrigable}} \tag{12}$$

where $h\_E(x,j)$ is the set of HRUs that have an AET of $x \pm \frac{1}{2}\Delta x$ on day j (here we use bins of width $\Delta x = 1$mm).

In order to help interpret the distribution of AET, we also consider the distribution of irrigation depths across the irrigable HRUs. This is summarized in a similar way to equation (12) by the area-weighted proportion of irrigable HRUs with a given AET, $\omega_j^{irrigated}(x)$,

$$\omega_j^{irrigated}(x) = \frac{\sum_{h \in h\_irrigated(x,j)} A_h}{A_j^{irrigable}} \tag{13}$$

where $h\_irrigated(x,j)$ is the set of HRUs that are irrigated to depth $x \pm \frac{1}{2}\Delta x$ on day j (here we use bins of width $\Delta x = 5$mm).

Two comparison days are selected to highlight differences in irrigation and simulated AET between the three irrigation schedule models: (i) a date when the SU-EB model simulated irrigation over all irrigated HRUs, and (ii) 5 days later, just before the next irrigation event occurs for SU-EB model.

Second, we consider how spatial variability in AET changes through time. For this purpose, spatial AET variability on a given day j is quantified using a "spatial coefficient of variation", $\mathrm{scv}E_j$, defined as the (weighted) standard deviation of AET values across the irrigable HRUs scaled by a "typical" AET over the analysis period, as given below:

$$\mathrm{scv}E_j = \frac{\mathrm{sdev}_w\left[\mathbf{E}_{\{h\_irrigable(j)\},j}; \mathbf{w}_{\{h\_irrigable(j)\}}\right]}{\mathrm{typ}E} \tag{14}$$

$$\mathrm{typ}E = \sum_{j \in \{j\_sel\}} \mathrm{ave}_w\left[\mathbf{E}_{\{h\_irrigable(j)\},j}; \mathbf{w}_{\{h\_irrigable(j)\}}\right] \tag{15}$$

Here $E_{h,j}$ represents the simulated AET at HRU h on day j, and the notation $\mathbf{E}_{\{h\_irrigable\},j} = (E_{h,j}; h \in h\_irrigable(j))$ denotes the AET values at the irrigable HRUs. The functions $\mathrm{ave}_w[]$ and $\mathrm{sdev}_w[]$ denote the weighted mean and weighted standard deviation, respectively (Gough, 2009), and the weights $\mathbf{w}$ are given by the HRU areas, i.e., $w_h = A_h$. The typical value of AET, typ$E$, is computed over a selected set of days $\{j\_sel\}$.

Note that, for the stochastic model SV-EB-RO, $\omega_j^E(x)$, $\omega_j^{irrigated}(x)$, and $\mathrm{scv}E_j$ are constructed using the first replicate; other replicates exhibit similar behavior and insight because equations (12)–(14) integrate over the HRUs and are sensitive to their aggregate properties rather than to the specific realizations.

Potential Recharge. Observations of potential recharge are not available, and hence our analysis is limited to making qualitative comparisons of potential recharge values simulated by SWAT with different irrigation schedule models.

5.3. Hydrological Model Parameters

As part of evaluating the streamflow response generated using the different irrigation schedule models, we consider the "flashiness" of the hydrograph, which is controlled by the surface lag coefficient (SURLAG) in SWAT. SURLAG lags a portion of the surface runoff release to the main channel and hence controls the fraction of surface runoff that is allowed to enter the stream on any given day (Neitsch et al., 2011). Higher values for SURLAG correspond to hydrographs with sharp peaks following rainfall events, while lower values exhibit slow decays after peaks. We compare the values of SURLAG calibrated given different irrigation inputs. Note that we do not attempt to interpret the influence of irrigation inputs on other calibrated SWAT parameters, because many parameters are poorly identifiable (see supporting information Section S1).

5.4. Uncertainty Evaluation

5.4.1. Total Simulation Uncertainty

The estimates of total uncertainty in hydrological simulations (section 4.3.1) are evaluated in terms of reliability and precision. Estimates of simulation uncertainty are considered reliable if the observed time series data are consistent with being samples from the distribution of total simulation uncertainty. The reliability metric of Evin et al. (2014) is used, which is based on the deviation of the predictive QQ plot (Thyer et al., 2009) from the 1:1 line. The reliability metric ranges between 0 (perfect reliability) and 1 (worst reliability, e.g., all data outside the simulation distribution).

Precision, often referred to as "sharpness" or "resolution," refers to the width or spread of the simulation uncertainty. In this study, precision is quantified using the coefficient of variation of the simulation replicates averaged over all the time steps (Evin et al., 2014). The precision metric ranges from 0 (perfect precision, i.e., no uncertainty) to large values (poorer precision, i.e., wide probability limits).

5.4.2. Partial Simulation Uncertainty

The relative contributions of irrigation schedule uncertainty (section 4.3.2) to the total simulation uncertainty in streamflow and AET (section 4.3.1) is estimated as the ratio of the average standard deviation of the simulated streamflow replicates associated with each source of uncertainty, i.e.,

$$\phi_k^{(\mathrm{irrig/total})} = \frac{\sum_{j=1}^{N_{j(k)}} \mathrm{sdev}\left[Y_{k,j}^{(\mathrm{sim,irrig})}\right]}{\sum_{j=1}^{N_{j(k)}} \mathrm{sdev}\left[Y_{k,j}^{(\mathrm{sim,total})}\right]} \tag{16}$$

Large values of $\phi_k^{(\mathrm{irrig/total})}$ correspond to irrigation uncertainty dominating total simulation uncertainty.

6. Results

6.1. Irrigation Time Series

6.1.1. Influence of Irrigation Schedule Model

We begin by comparing simulated irrigation time series at the HRU and catchment scales for the four irrigation schedule models described in section 2. For the SV-EB models, we consider only small HRUs (section 3.3.3) and use multiple stochastic replicates. Figure 4 plots simulated irrigation for a single HRU characterized by a crop type that is irrigated during the Austral summer (November–February).

As expected, Figure 4a shows that ignoring spatial and temporal variability (SU-C) leads to small irrigation depths, ~5 mm/day, being simulated on each day. In contrast, incorporating event-based irrigation, while still ignoring spatial variability (SU-EB), produces discrete irrigation events, with intervals between irrigation events of the order of 10 days, and (by construction) irrigation depths per single event of approximately 50 mm. The SU-EB simulations are clearly more consistent with BMPs described in section 3.2.

Figure 4b shows that the HRU scale irrigation given by the individual replicates of SV-EB-RT model are similar to each other and to the SU-EB model in Figure 4a. They all simulate irrigation depths of 50 mm (again by construction), and irrigation intervals of ~10 days. However, the timing (dates) of the irrigation events are

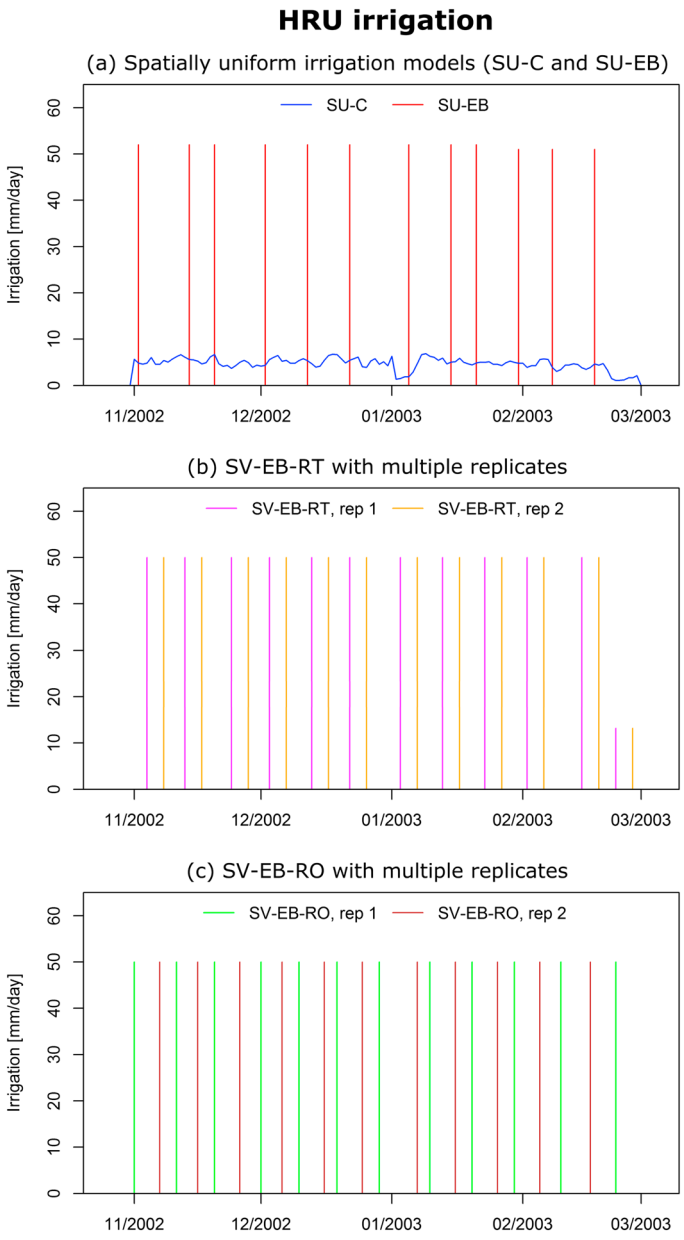

Figure 4. Simulated irrigation for a single HRU with a summer-irrigated crop type, obtained using the irrigation schedule models.

different. The SU-EB model simulates irrigation at the end of each irrigation interval, while the SV-EB-RT model simulates irrigation at a random day within the first irrigation interval, and then on the same day within subsequent intervals.

Figure 4c shows two replicates of irrigation at the HRU scale for the SV-EB-RO model, illustrating that it is similar to the SU-EB and SV-EB-RT models in terms of irrigation depths and intervals, but different in the timing of events.

In terms of total water (combined rain and irrigation) applied to HRUs with perennial pasture irrigated spring-to-autumn (section 3.2.2), all three irrigation schedule models simulate annual values in the range of 1,250–1,300 mm (results not shown). The slight variability arises due to the different irrigation schedule models; the SV-EB-RO model irrigates the HRUs in a predefined order, so some HRUs receive an extra event than other HRUs, whereas this is not the case for the SU-C and SU-EB models. The range of 1,250–1,300 mm matches very closely the recommended value of 1,300 mm listed in section 3.2.2. Such a close match is perhaps unexpected given the data and modeling uncertainties involved, but could be an indirect indication of a general agreement between the total water amounts ordered by the farmers (and used as total catchment irrigation input in our models) and the total water requirements (rain and irrigation) estimated by Victorian Resources Online (2017). Note that we could not conduct a similar analysis over HRUs of other crop types due to data limitations (section 3.2.2).

Figure 5 shows the observed and simulated catchment irrigation over the simulation period between August 2002 and June 2003. The observed rainfall is also shown in Figure 5a.

Figure 5b confirms that (by construction) the SU-C model simulates catchment irrigation that matches the observations exactly. In contrast, the event-based (but spatially uniform) SU-EB model simulates catchment irrigation that is much peakier than the observed time series. Whereas the observed catchment irrigation varies minimally from day to day, with a maximum depth of ~2 mm/d, the simulated catchment irrigation from the SU-EB model is zero on most days, with occasional days with extremely large catchment irrigation of up to 45 mm.

Figure 5c evaluates the spatially variable event-based irrigation simulated using the SV-EB-RT model. It is clear the SV-EB-RT model fits the observed irrigation data better than the SU-EB model (Figure 5b). However, the SV-EB-RT model still incurs notable differences from the observed time series: some days have zero catchment irrigation, whereas on other days the simulated depths far exceed the observed depths. Furthermore, the SV-EB-RT irrigation schedule model does not reproduce the dips in observed catchment irrigation following rainfall events, when there is little to no irrigation (e.g., at the start of January 2003, as shown in Figure 5a).

Simulated catchment irrigation from the SV-EB-RO model (Figure 5d) matches the observations better than the SV-EB-RT model (Figure 5c). Another advantage of the SV-EB-RO model over SV-EB-RT model is that the differences between the replicates themselves are smaller.

These results show that even though observed daily catchment irrigation is used as an input to all four irrigation schedule models, there are substantial differences in the corresponding simulations of daily HRU and catchment irrigation. Overall, the irrigation model SV-EB-RO, which assumes spatially variable

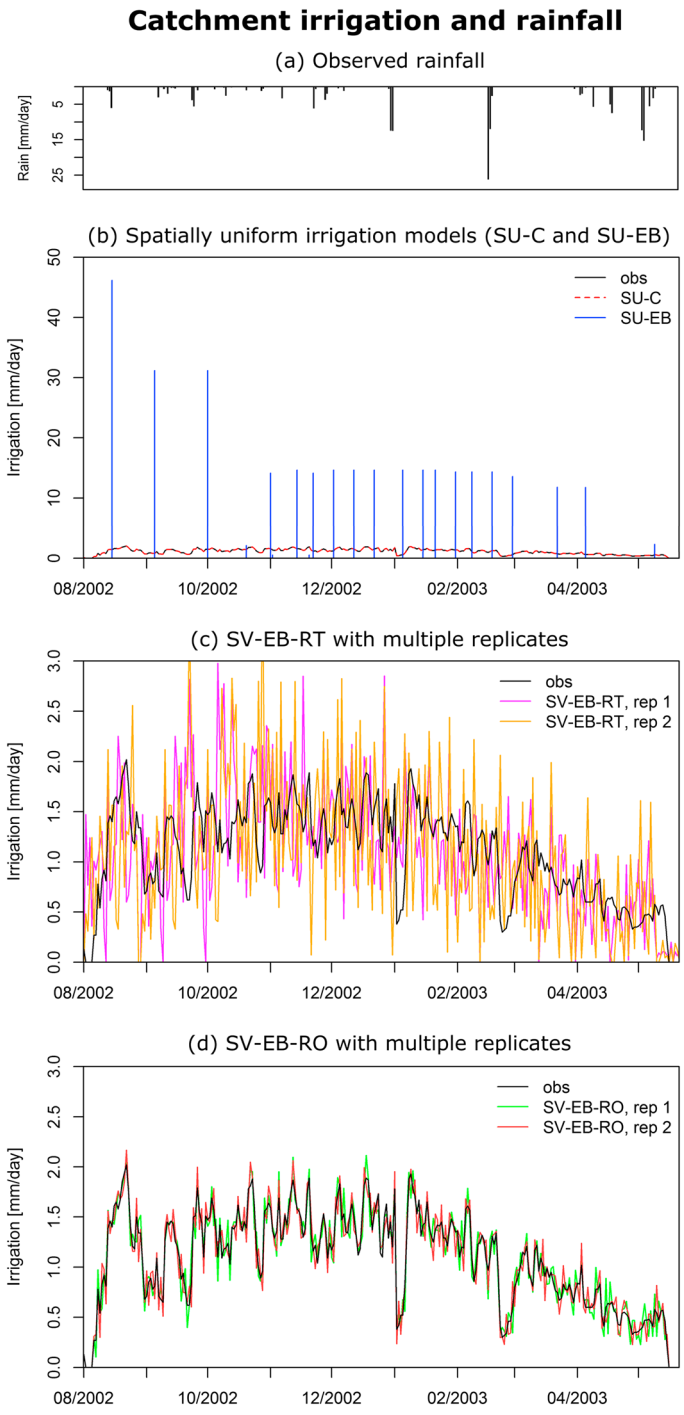

Figure 5. Observed and simulated catchment irrigation obtained using the irrigation schedule models. The SV-EB models are applied with small HRUs. For the stochastic models SV-EB-RT and SV-EB-RO, two representative replicates, labeled as "rep 1" and "rep 2," are shown. Observed rainfall is also shown.

event-based with random ordering, is the only irrigation schedule model that matches both (i) Best Management Practices (irrigation depths and intervals) at the HRU scale and (ii) observed irrigation data at the catchment scale. This finding will be discussed in section 7.1.

6.1.2. Influence of Spatial Discretization

Next we compare the impact of spatial discretization on irrigation schedules. Figure 6 compares the effect of (i) the choice of spatially variable event-based irrigation schedule model (SV-EB-RT versus SV-EB-RO), and (ii) the size of the HRUs (large versus small), on simulated catchment irrigation. In both models, the use of large HRUs yields simulated catchment irrigation that is spikier and less accurate compared to observations than when small HRUs are used. Reducing the size of HRUs to better match the typical spatial scale of farms in Victoria, Australia (section 3.2.1) results in smaller spikes in the simulated catchment irrigation. This is discussed further in section 7.1.2.

6.2. Hydrological Model Simulations and Parameters

This section reports simulated responses and calibrated parameters when SWAT is forced with: (i) spatially uniform continuous-time irrigation (SU-C), (ii) spatially uniform event-based irrigation (SU-EB), and (iii) 10 replicates from the spatially variable event-based model with random order (SV-EB-RO), with the smaller HRU size. The SV-EB-RT model is excluded from this analysis because it is in the same class as the SV-EB-RO model in terms of producing spatially variable and event-based irrigation, but produces less accurate daily catchment irrigation (section 6.1.1).

Figure 7 shows SWAT streamflow simulations at the catchment and subcatchment outlets, Figure 8 compares SWAT simulations of AET and potential recharge, and Table 2 summarizes performance based on the metrics in section 5.2. The overall water balance of the SWAT simulations is reported in Table S2 and discussed in Section S2 of the supporting information.

Forcing SWAT with SU-EB irrigation inputs produces simulated hydrographs that poorly capture the fast response to rainfall events: they exhibit smaller peak flows and much slower recessions than the observed hydrograph (Figures 7b and 7c). In contrast, the use of the SU-C and SV-EB-RO model inputs in SWAT produces simulated hydrographs that better capture the fast response to rainfall events. This results in the SU-C and SV-EB-RO models leading to more accurate daily streamflow simulations at the catchment and subcatchment outlets than when the SU-EB model is used (Table 2). For example, at the catchment outlet, using the SU-C and SV-EB-RO model results in daily streamflow NSE values of ~0.9 and NSE-SA values of ~0.55, compared with an NSE of ~0.8 and NSE-SA of ~0.15 when the SU-EB model is used.

The optimal values of the SWAT parameter SURLAG (see section 5.3) are consistent with these findings; for the SU-EB model the optimal SURLAG value is 0.14, resulting in the slower response in SWAT simulated streamflow; when the SU-C and SV-EB-RO model are used optimal values for SURLAG are 1.1 and 1.3, respectively, resulting in much faster responses to rainfall events.

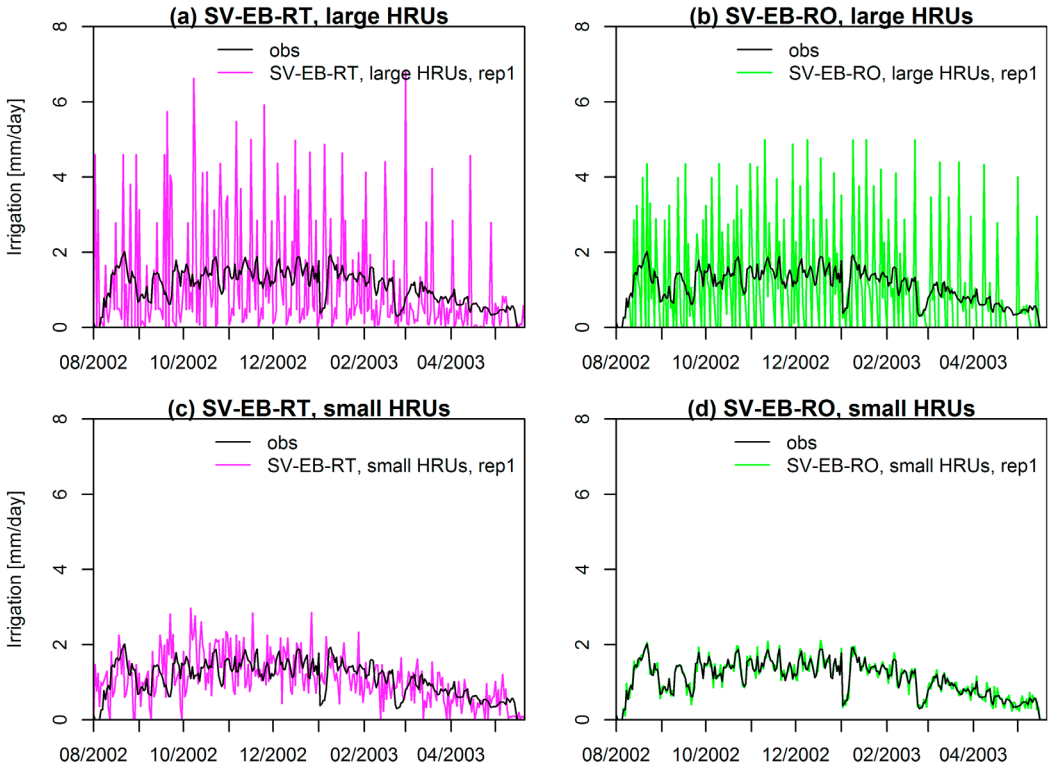

Figure 6. Effect of spatial discretization (large versus small HRUs) on catchment irrigation simulated using irrigation schedule models SV-EB-RT and SV-EB-RO.

Differences in other SWAT parameter values are not interpreted in this study (see supporting information Section S1).

In terms of AET, when the continuous-time (SU-C) irrigation inputs are used, SWAT over-estimates monthly catchment AET, which results in a poor NSE (−0.17) and large positive bias (+37%) as reported in Table 2. These biases are much larger than the 10–20% observation errors expected for the remotely sensed AET data (section 3.2). However, when event-based SU-EB and SV-EB-RO models are used, SWAT yields monthly AET estimates with much better NSE (0.71 and 0.56, respectively) and much smaller biases (+4.8% and +1.7%).

The large differences in SWAT AET estimates when continuous-time irrigation inputs (SU-C) are used in lieu of event-based irrigation inputs (SU-EB and SV-EB-RO) translate into large differences in simulations of potential recharge. While the SU-EB and SV-EB-RO models lead to similar SWAT simulations of potential recharge (mean values of ~19 mm/month), the use of the SU-C model produces much lower simulations (mean value of ~9 mm/month).

Next we consider the impact of spatiotemporal variability in irrigation inputs on the spatial variability in AET, using the methods described in section 5.2. We focus on the heavily irrigated period of November 2002 to February 2003, and report the spatial variability over irrigable HRUs in that period. Figure 9, columns 1 and 2, show the distributions of irrigation and AET, quantified using $\omega^{irrigated}$ and ω^{E} from equations (13) and (12) respectively, on the 15 January 2003—a day on which the SU-EB model simulates an irrigation event. Similarly, columns 3 and 4, show distributions of irrigation and AET, but for the 20 January 2003—5 days after the irrigation event simulated by the SU-EB model. Finally, column 5, shows how the spatial variability in AET changes in time for each day between November 2002 and February 2003, quantified using the scv*E* metric in equation (14).

Under SU-C model assumptions, all irrigable HRUs receive the same small amount (~5 mm/d) of irrigation on a given day (columns 1 and 3). As a consequence, the variability in AET is low, with all irrigable HRUs having

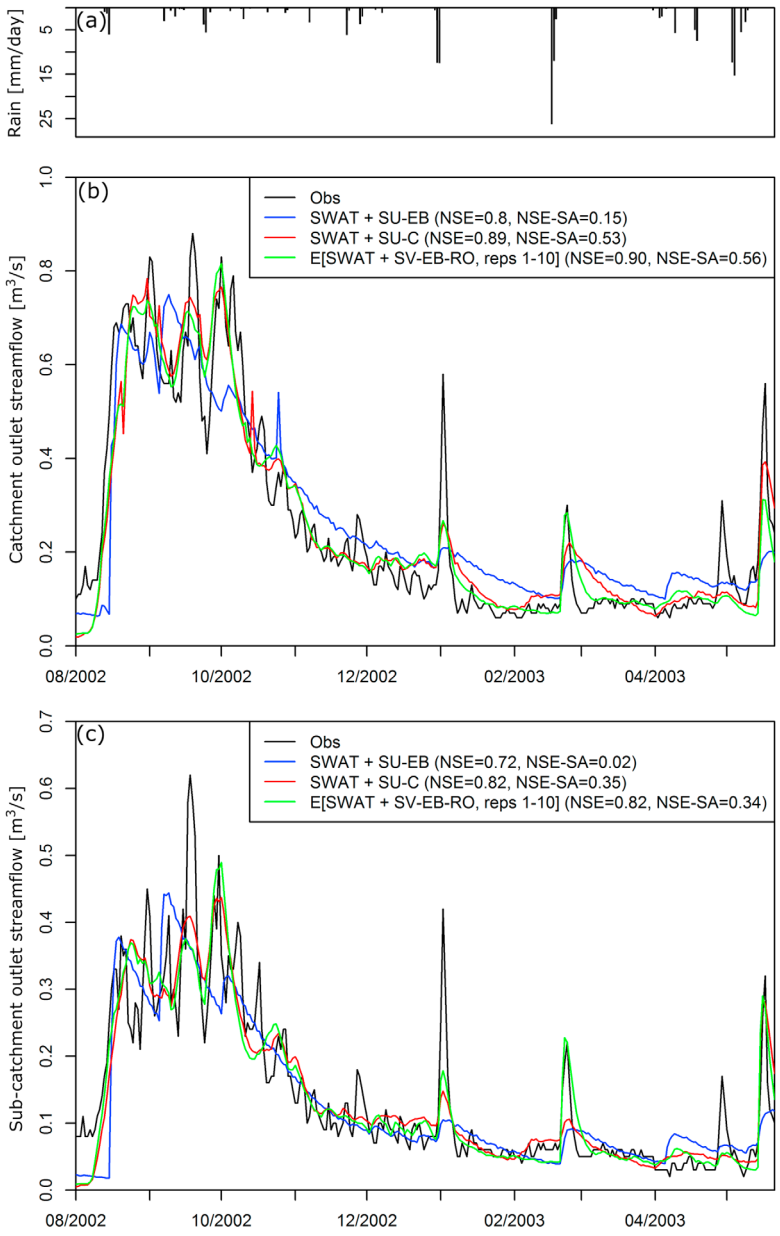

Figure 7. Evaluation of streamflow simulations obtained using SWAT forced with irrigation schedule models SU-C, SU-EB, and SV-EB-RO (replicates 1–10). For the SWAT calibration using multiple irrigation replicates, the expected value of the SWAT streamflow is shown.

similar AET of around 5–6 mm/d. Note that this AET value is fairly high because water is always available for evaporation. The low spatial variability in AET is seen in columns 2 and 4 for specific dates, and in the summary column 5 where the average value of scv$E$ is 0.04. This minor variability is likely due to differences in AET from different crop types and different soil types.

Under SU-EB model assumptions, all irrigable HRUs receive either a large amount of irrigation (~50 mm/d) on the same day, or no irrigation at all, as seen in columns 1 and 3, respectively. In other words, similar to the SU-C model, there is no spatial variability in irrigation. On days when irrigation is applied, AET is around 5 mm/d over all irrigable HRUs and has little spatial variability (column 2). However, 5 days after the irrigation event has occurred, spatial variability in AET increases (column 4), with 40% of irrigable HRU having no AET. This dynamic appears related to the soil properties—heavy and medium clay have higher AET, while light

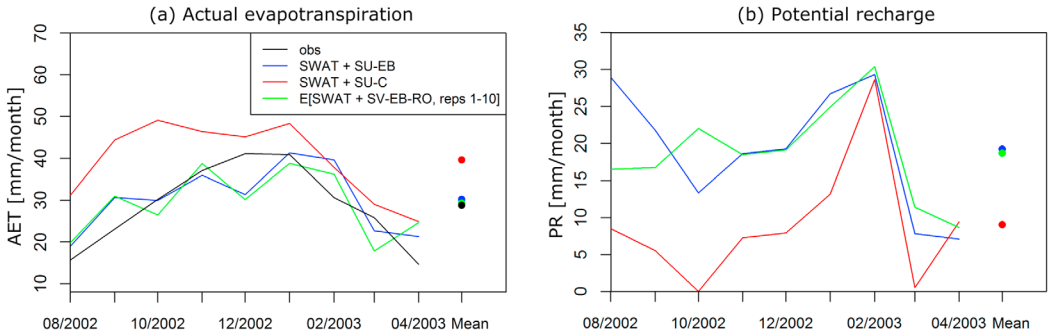

Figure 8. Monthly catchment scale actual evapotranspiration (AET) and potential recharge obtained using SWAT forced with irrigation schedule models SU-EB, SU-C, and SV-EB-RO (replicates 1–10). Dots represent mean values over all months within the simulation period. For AET, observed data are available and shown.

soils have low AET. We speculate that AET is lower in light soils due to water draining and becoming unavailable for evaporation—a behavior that does not occur in heavy soils. For this reason, even though both the SU-C and SU-EB models simulate spatially uniform irrigation, the SU-EB model results in a much more spatially variable AET. For example, even though on some days the scv*E* corresponding to the SU-EB model is close to 0 (similar to the SU-C model), on other days it increases to nearly 1. Over the entire period, scv*E* has a mean ~0.4 when the SU-EB model is used, which is 10 times higher than when the SU-C model is used.

The SV-EB-RO model introduces spatial variability in irrigation *and* reflects its event-based nature. Columns 1 and 3 show that, on these selected days, a small proportion (~10%) of irrigable HRUs receive the nominal daily amount of 50 mm, and the remaining areas receive no irrigation. The spatial variability in irrigation leads to large spatial variability in AET: around 40% of irrigable HRUs have no AET, and the remaining 60% have AET of approximately 3–7 mm/d (column 2) and 2–10 mm/d (column 4). Column 5 shows that the SV-EB-RO model leads to more spatial variability of AET than the SU-EB and SU-C models, with an average scv*E* of 0.82, i.e., twice higher than the SU-EB model and 20 times higher than the SU-C model. Note that there are a few days when spatial variability in AET is low (column 5); these days typically follow rainfall events (e.g., early January 2003), when all HRUs receive a similar amount of water and hence there is less spatial variability in the inputs.

The differences in hydrological simulations and parameters due to differences in spatiotemporal variability will be discussed in section 7.1.

Table 2
Performance Metrics of Hydrological Response Simulations and Estimated Simulation Uncertainty, for SWAT Model Applications Driven by Different Irrigation Schedule Models

		Irrigation schedule models		
		SU-C	SU-EB	SV-EB-RO, reps 1–10
Catchment outlet daily streamflow	NSE	0.89	0.80	0.90
	NSE-SA	0.53	0.15	0.56
	Reliability	0.14	0.27	0.09
	Precision	0.32	0.45	0.31
Subcatchment outlet daily streamflow	NSE	0.82	0.72	0.82
	NSE-SA	0.35	0.02	0.34
	Reliability	0.08	0.11	0.04
	Precision	0.35	0.54	0.33
Monthly AET	NSE	−0.17	0.71	0.56
	Bias (%)	+37	+4.8	+1.7

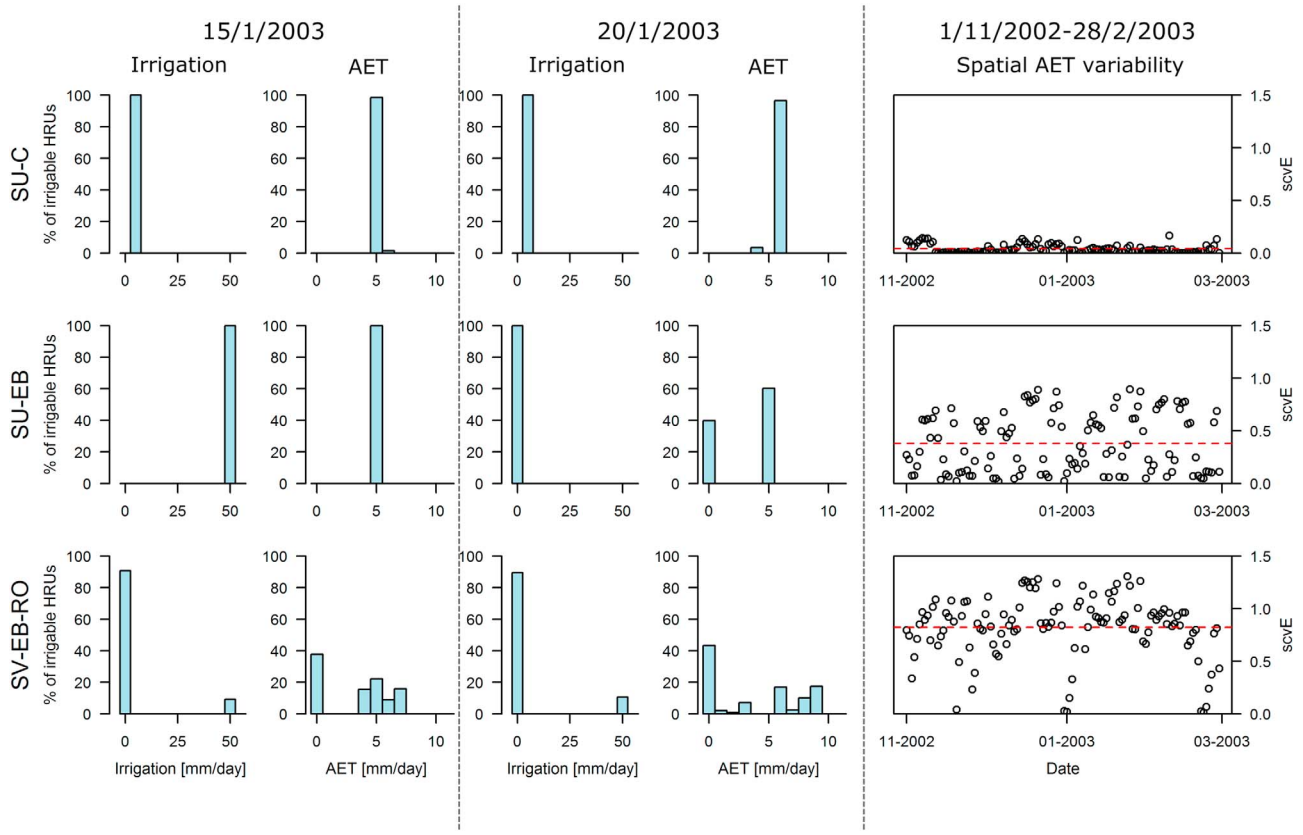

Figure 9. Spatial variability in simulated irrigation and AET. The three rows correspond to the three irrigation schedule models, with the SV-EB-RO model results being represented by its first replicate. Spatial variability is depicted using the distributions of irrigation depths and AET amounts on a given day (quantities $\omega^{irrigated}$ and ω^{E} shown in columns 1–4), and by the spatial coefficient of variation of AET over the entire analysis period (quantity scv$E$ shown in column 5). Columns 1–2 show the results on 15 January 2003, and columns 3–4 show the results from 5 days later, i.e., on 20 January 2003.

6.3. Uncertainty in Simulations

6.3.1. Total Simulation Uncertainty

Figure 10 shows the total simulation uncertainty in streamflow at the catchment and subcatchment outlets, and Figure 11 shows total simulation uncertainty in catchment AET, when SWAT is forced by the SU-C, SU-EB and SV-EB-RO models. Table 2 summarizes the performance metrics for reliability and precision based on the metrics described in section 5.4.1.

In terms of simulation uncertainty in streamflow, the following findings are noted:

1. *Reliability*. The inclusion of spatiotemporal variability in irrigation inputs leads to the most reliable estimates of simulation uncertainty in streamflow. The SV-EB-RO model leads to reliability metrics of 0.09 and 0.04 at the catchment and subcatchment outlets, respectively. Ignoring spatial variability (SU-EB) results in the worst reliability (reliability metrics of 0.27 and 0.11); ignoring both spatial and temporal variability (SU-C) also provides inferior results (reliability metrics of 0.14 and 0.08).
2. *Precision*. The inclusion of spatiotemporal variability in irrigation inputs leads to the best precision in simulated streamflows. The SV-EB-RO model leads to precision metrics of 0.31 and 0.33 at the catchment and subcatchment outlets, respectively (Table 2). Ignoring spatial variability (SU-EB) results in the worst precision (precision metrics of 0.45 and 0.54), while ignoring both spatial and temporal variability (SU-C) also provides (slightly) worse results (precision metrics of 0.32 and 0.35).

In terms of simulation uncertainty in AET, due to the small number of data points available we do not report the reliability and precision metrics. Visual inspection of the time series in Figure 11 suggests a similar pattern to the deterministic results reported previously in Figure 8: SWAT captures the observed AET better when the irrigation inputs are generated by the event-based SU-EB and SV-EB-RO models rather than by the continuous-time SU-C model.

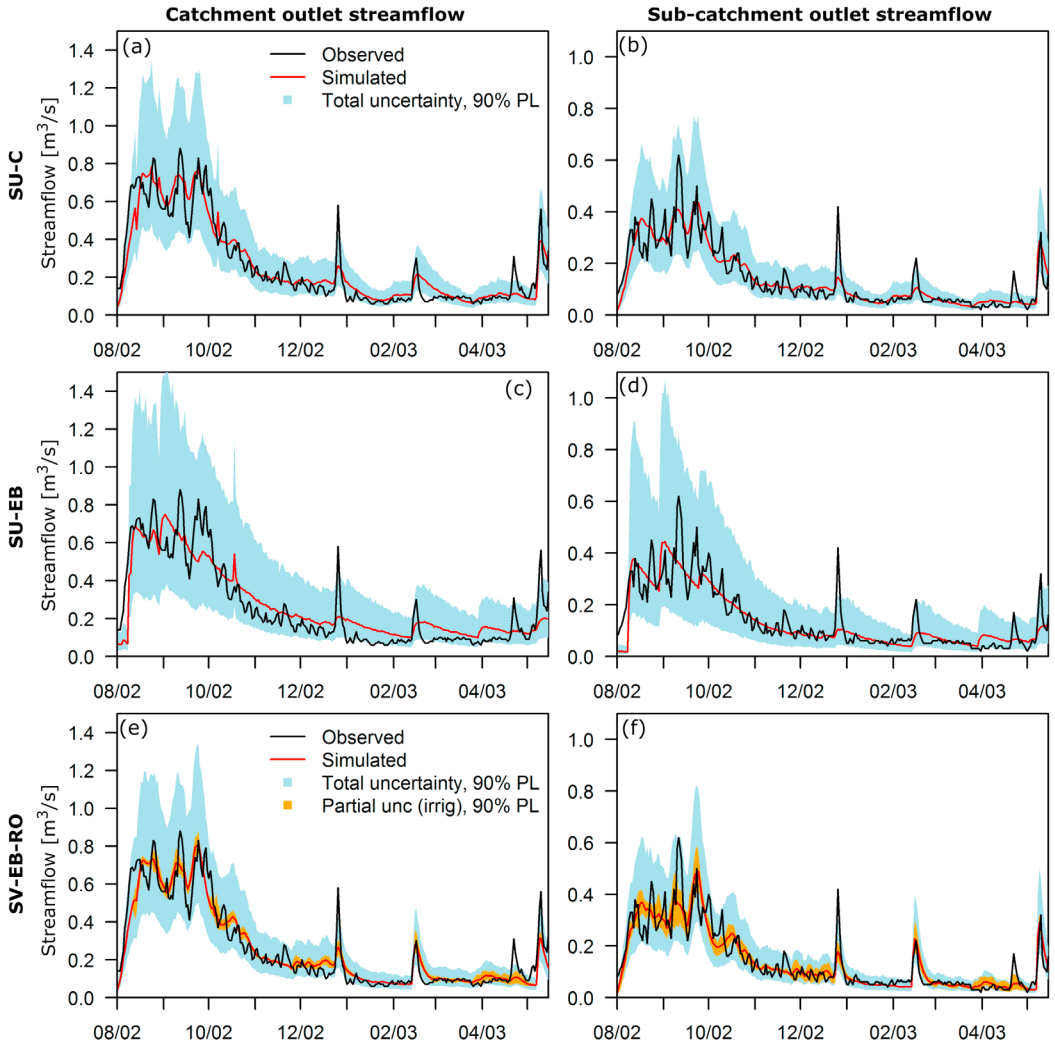

Figure 10. Total simulation uncertainty in catchment and subcatchment outlet streamflow obtained using SWAT forced with SU-C, SU-EB, and SV-EB-RO irrigation. The contribution of irrigation schedule uncertainty to total simulation uncertainty is also shown for the SV-EB-RO model. Estimated uncertainty ranges (total streamflow uncertainty and partial streamflow uncertainty due to irrigation uncertainty alone) are shown using 90% probability limits.

6.3.2. Irrigation Schedule Uncertainty (SV-EB-RO Model Only)

This section quantifies the uncertainty in hydrological simulations directly attributable to the uncertainty in the SV-EB-RO irrigation inputs by considering the SWAT response to the individual replicates of this irrigation schedule model. These results are shown in Figures 10e and 10f and 11c.

For the case of catchment outlet streamflow, Figure 10e shows that the uncertainty range due to irrigation input uncertainty is relatively small, around 20% of the total simulation uncertainty. In contrast, the effect of irrigation schedule uncertainty on subcatchment streamflow is much larger, as seen by the probability limits in Figure 9f being considerably wider than in Figure 10e. In terms of quantitative estimates, approximately 40% of total simulation uncertainty at the subcatchment streamflow is attributed to irrigation schedule uncertainty. This finding will be discussed in section 7.2. The relative contribution of irrigation input uncertainty to total simulation uncertainty is largest during low rainfall periods, when the relative ratios of irrigation to rainfall volumes are largest. Note that these periods tend to be characterized by low flows.

For AET, the effect of irrigation schedule uncertainty is negligible, as shown in Figure 11c. This behavior is likely due to the monthly averaging required to compare simulations with observed values.

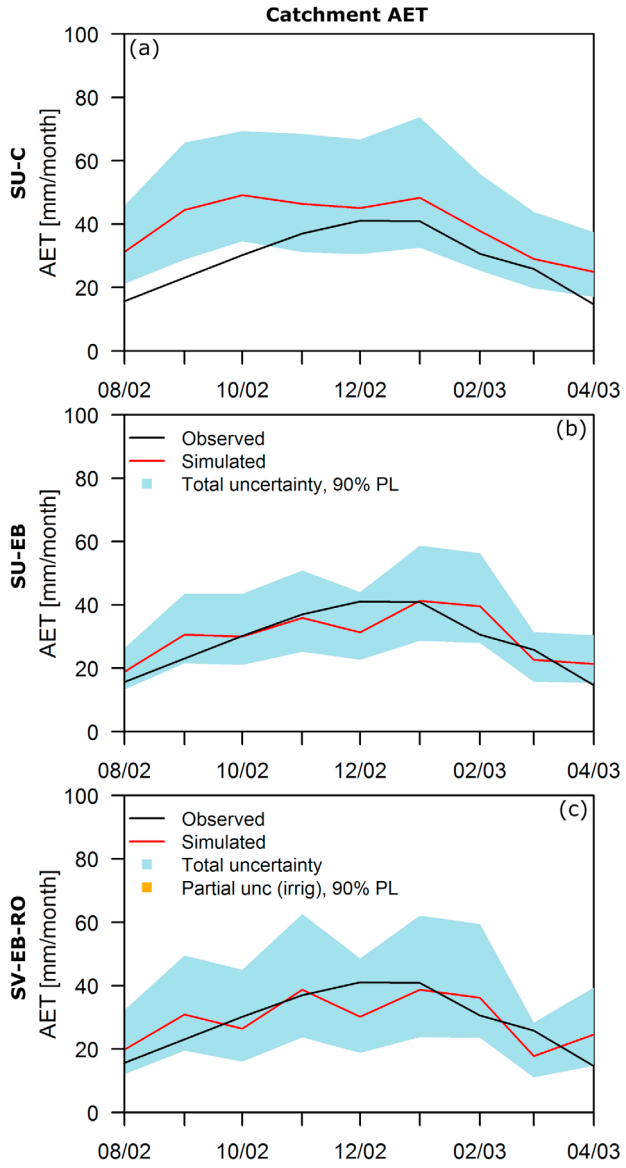

Figure 11. Total simulation uncertainty in monthly catchment AET obtained using SWAT forced with SU-C, SU-EB, and SV-EB-RO models. The partial uncertainty, i.e., the contribution of irrigation schedule uncertainty to total simulation uncertainty, for the SV-EB-RO model is also plotted, but is very small and not visible behind the red line.

More generally, Table S2 in the supporting information shows that, when the SV-EB-RO irrigation model is used, irrigation schedule uncertainty has negligible impact on the contributions of AET, recharge and streamflow to the catchment total water balance as simulated by SWAT.

These results suggest that the impact of irrigation schedule uncertainty on the total simulation uncertainty in hydrological quantities such as streamflow and AET depends on the spatial and temporal scale of interest. This finding will be discussed in section 7.2.

7. Discussion

7.1. Importance of Irrigation Schedule Model

7.1.1. Representing Spatiotemporal Variability

In this work, model irrigation inputs are provided at the scale of the catchment. The SU-C model ignores subsampling-scale spatial and temporal variability in irrigation inputs. This model produces smoothly varying irrigation time series at the catchment scale that (by construction) match the observed values, but (unsurprisingly) produces unrealistically low irrigation depths applied each day at the HRU scale. Despite its lack of spatiotemporal variability, the SU-C model leads to relatively good simulations and simulation uncertainty of daily streamflow, which we attribute to this model correctly reproducing the daily catchment total irrigation. However, the application of unrealistically small irrigation depths precludes enough infiltration from occurring, and subsequently most of the water from irrigation evaporates from the upper soil layer, resulting in a simulated AET well in excess of observed values (Figure 8). Note that the over-estimation of simulated AET occurs *despite* observed AET being used in the SWAT calibration. Similar over-estimation of AET was found during exploratory testing with increased weights for AET errors in equation (3), such that AET contributed to ~95% of the weighted sum of squared errors, compared with ~5% for the calibration setup reported in Figure 8. Since AET is the dominant component of the water balance (see section 3.1 and supporting information Section S2), simulations of other components of the hydrological cycle (e.g., potential recharge) are subsequently affected by these biases in simulated AET.

The SU-EB model implements event-based irrigation while ignoring subsampling variability in space. Under these assumptions, the simulated irrigation at the HRU scale provides a good match to the Best Management Practices in terms of irrigation depths and intervals (Figure 4a). However, as seen in Figure 5b, the SU-EB model does not reproduce the observed daily catchment irrigation, even when it is a given input: it simulates unrealistically high peaks in irrigation at the catchment scale (i.e., too many days with no simulated catchment irrigation, and too many days where simulated catchment irrigation is an order of magnitude larger than observed). This is a clear limitation of the SU-EB model—the spatial uniformity of the event-based irrigation results in large areas of the catchment being irrigated on the same day.

The spatial uniformity of irrigation inputs simulated by the SU-EB model substantially degrades the resulting SWAT calibration, leading to simulated streamflow time series that are much smoother than the observations. Figure 7 shows that the unrealistically high peaks in simulated catchment irrigation are not followed by large peaks in observed streamflow. The calibration process then attempts to suppress the spikiness of simulated streamflow by favoring parameter values that produce exceedingly slow-responding dynamics. This behavior is seen in the calibrated SURLAG parameter, which takes much lower values (0.14 days) when the SU-EB model is used compared to when the SU-C and SV-EB-RO models are used (1.1 and 1.3 days, respectively). The SWAT model calibrated with SU-EB irrigation produces a mediocre fit to the streamflow during irrigation events, and is completely unable to reproduce the fast streamflow response to rainfall events (see Figure 7).

Essentially, the calibration forces the hydrological model parameters to compensate (rather imperfectly) for poor quality inputs during particular time periods—ironically, sacrificing performance during time periods when inputs are more accurate.

The event-based nature of the SU-EB model provides a clear improvement over the continuous-time (SU-C) model in terms of AET simulations. This demonstrates the importance of event-based irrigation at the HRU scale on estimates of AET. Event-based irrigation allows more infiltration to occur, and subsequently less water evaporates. As a result, AET simulations based on using SU-EB irrigation inputs in SWAT have low overall bias, compared with those based on SU-C irrigation.

The SV-EB-RO, which allows for subsampling-scale spatial variability and event-based irrigation, matches the best performance aspects of the spatially uniform continuous-time (SU-C) and spatially variable event-based (SU-EB) models. The SV-EB-RO model provides accurate deterministic simulations, as well as reliable and precise probabilistic streamflow simulations—because, similar to the SU-C model, it accurately reproduces catchment irrigation. But the SV-EB-RO model also results in AET estimates with low overall bias—because, similar to the SU-EB irrigation schedule model, it reproduces the temporal variability of irrigation at the HRU scale.

7.1.2. The Need for Careful Implementation of the SV-EB Irrigation Schedule Model

Spatially variable event-based (SV-EB) irrigation is required to produce simulated irrigation that both varies smoothly at the catchment scale, and matches Best Management Practices at the HRU scale in terms of the approximate irrigation intervals and depths. However, the specific implementation of the SV-EB irrigation schedule model is important. For example, the catchment irrigation simulated by the SV-EB-RT model does not match the observed catchment irrigation (Figure 5c)—despite receiving the observed daily catchment irrigation as an input. This inconsistency arises because in the SV-EB-RT model the irrigation event is randomly selected from the first simulated irrigation interval; in contrast, the SV-EB-RO model is designed by construction to closely match the observed daily catchment irrigation.

The size of the HRUs used in the SV-EB-RO model is also important. By reducing the HRUs to more closely match typical farm sizes, we reduce the volume of water required in the model to irrigate the largest HRU on a single day, and hence reduce the large spikes in daily simulated catchment irrigation.

7.1.3. Implications for Practical Use of Distributed Models

The spatially variable event-based (SV-EB-RO) irrigation schedule model recommended in this work includes both spatial and temporal variability, and requires a relatively small HRU size commensurate with typical farm-scales (sections 3.3.3 and 6.1.2). This finding agrees with the general idea that the spatial discretization of an environmental model should reflect the spatial scales of the dominant system dynamics. In view of the large portion of catchment inputs contributed by irrigation (supplementary information Table S2), irrigation practices at the farm-scale and spatial variations thereof can substantially affect catchment water balance dynamics. For this reason, as seen in the comparison of irrigation simulations under "small HRU" versus "large HRU" assumptions, farm size information is relevant for defining HRUs and for successful streamflow modeling at the catchment scale.

More broadly, the case study illustrates the value of multivariate data in model hypotheses testing, and the direct relevance of the modeling objectives to the model evaluation process (e.g., Clark et al., 2011). Had we evaluated hydrological simulations solely against observed streamflow and overlooked diagnostics against observed AET, we may have concluded that the SU-C and SV-EB-RO models both produce sufficiently adequate irrigation inputs (Figure 7). However, these two irrigation inputs lead to very different estimates of potential recharge (Figure 8b). When observed AET is used to evaluate the hydrological model, the advantages of the SV-EB-RO model become evident (Figure 8a). Since AET is such a large component of the overall water balance (section 3.1 and supporting information Table S2), we have more confidence in the estimates of potential recharge (as well as in other AET-dependent model responses, such as crop yields) obtained using the SV-EB-RO model rather than the SU-C model.

In contrast, if the modeling objective was solely to provide accurate streamflow predictions, the results in section 6.2 suggest that spatial and temporal variability in irrigation inputs is less important, and the simple SU-C model may suffice. This finding is consistent with the use of spatially averaged rainfall to force lumped rainfall-runoff models, which is common in research and operational practice (e.g., Bergström, 1995; Perrin et al., 2003; Tuteja et al., 2012).

7.2. Impact of Irrigation Schedule Uncertainty on Hydrological Simulations

The ability to decompose total simulation uncertainty into its contributing sources is an important benefit of the calibration and simulation framework used in this study. The results suggest that the spatial scale of

interest (subcatchment or catchment) affects the contribution of irrigation schedule uncertainty to total simulation uncertainty. At the subcatchment outlet, irrigation schedule uncertainty contributes ~40% of total streamflow uncertainty, whereas at the catchment outlet this contribution decreases to around ~20%. There are several potential reasons for this finding: (i) multiple replicates of subcatchment irrigation are much more variable than the corresponding replicates of catchment irrigation itself, because the latter is (substantially) constrained by the observed values (Figure 5d); (ii) the streamflow at larger spatial scales averages out variations in irrigation, (iii) this particular subcatchment has the most irrigated land of all subcatchments, so that irrigation not only makes up a larger proportion of total inputs (rain plus irrigation), but total inputs are more uncertain.

The pragmatic approach adopted in this study to incorporate the influence of irrigation schedule uncertainty is based on the expected value of SWAT simulations averaged over multiple replicates of irrigation inputs. Therefore, this approach does not directly incorporate irrigation uncertainty into the hydrological simulations, does not include data uncertainty in the observed AET or streamflow, and does not include parameter uncertainty in the hydrological model. An alternative approach would be to use a complete Bayesian hierarchical representation, such as the Bayesian Total Error Analysis (BATEA) framework (Kavetski et al., 2006; Renard et al., 2011). The expectation-based approach in equation (4) was favored in this study due to its lower computational demand—which is a critical consideration given the typical SWAT model runtime of 5–6 s as opposed to the typical runtime of the GR4J model used by Renard et al. (2011) being 10^{-2} s. Future work using BATEA could investigate the characterization of all major sources of error including hydrological model, parameter, and data uncertainty (including irrigation schedule uncertainty).

Finally, the use of stochastic models to represent subscale variability and resulting uncertainty in data is common in environmental applications (e.g., Kandel et al., 2005). This study supports the value of this approach—we are able to construct a stochastic model of spatially variable irrigation inputs, using a combination of spatially aggregated data (observed catchment irrigation) and general insights into subscale variability (in this case, an understanding based on Best Management Practices). This approach improves the quality of hydrological simulations, compared to approaches that ignore some aspect of this subgrid variability (e.g., spatial uniformity or continuous-time).

7.3. Future Research in Irrigation Schedule Modeling

Further improvement of irrigation schedule models could proceed along the following directions:

1. *Include Additional Information on Farm-Scale Irrigation Water Use*. Irrigation water use data at the farm-scale and/or higher resolution AET at the farm-scale could enable more incisive model evaluation and improve the spatiotemporal irrigation models. The assumption that crops receive a fixed irrigation depth of 50 mm per event, and that irrigation intervals are the same for each crop, could be relaxed by varying these parameters, e.g., using the approach of Connell et al. (2001) for specifying irrigation parameters. Future research could also explore the benefits (if any) of refining HRU sizes to match actual irrigated subareas within particular farms.
2. *Improve Representation of the Irrigation Water Supply System*. This study ignored the uncertainty in daily catchment irrigation data (taken as 60% of estimated daily offtake in the No. 1 Channel in accordance to annual irrigation volumes) and the delay caused by irrigation channel routing between the No. 1 Channel offtake and the farms. Addressing these limitations could improve the quality of hydrological simulations.
3. *Extended Evaluation of the Role of Irrigation Schedule Inputs on Distributed Models*. Due to limitations of available data for the case study catchment considered in this study, SWAT was calibrated to only 9 months of data, and simulation performance was assessed only over this calibration period. Further work is required to assess the robustness of our findings, including the attribution of uncertainties, over an independent evaluation period. In addition, future research is warranted to transfer the insights on spatiotemporal variability in irrigation inputs to other simulated responses (e.g., hydrological, environmental, and agricultural responses), catchments, and distributed hydrological models, including the "Source" models applied in the Murray Darling Basin in Australia (MDBA, 2017).

8. Conclusions

Distributed hydrological models are increasingly used to inform the management of agriculturally important irrigated catchments. This study evaluated the importance of spatiotemporal variability in irrigation inputs on simulations of major hydrological processes, including streamflow, actual evapotranspiration and potential

recharge. A case study based on an application of the SWAT hydrological model to an irrigated catchment in the Murray Darling Basin in Victoria, Australia was reported. We evaluated four irrigation schedule models differing in their representations of spatiotemporal variability of irrigation depth, including spatially uniform continuous (SU-C), spatially uniform event-based (SU-EB) and spatially variable event-based (SV-EB) models.

A new spatially variable event-based model (SV-EB-RO) based on random ordering of irrigated HRUs was developed to better match observed catchment irrigation than an existing spatially variable event-based model (SV-EB-RT) based on random timing of irrigation events.

The case study results highlight the importance of capturing the spatiotemporal variability of irrigation inputs for obtaining accurate simulations of streamflow and actual evapotranspiration. More specifically:

1. Including both spatial and temporal variability in irrigation using the SV-EB-RO model provides the best simulations of daily streamflow and monthly AET. The improved performance of the SV-EB-RO model is attributed to its ability to generate event-based irrigation events at the HRU scale (unlike the SU-C model) but smooth irrigation time series at the catchment scale (unlike the SU-EB model).
2. When spatial variability at the HRU scale is ignored but event-based temporal variability is included (SU-EB model), very poor quality simulations of daily catchment streamflow are obtained. Under these circumstances, the irrigation time series at the catchment scale are unrealistically peaky, and the calibrated hydrological parameters attempt to compensate for this model mismatch by producing a muted hydrological response. This reduces the daily streamflow NSE-SA from 0.53 when the SV-EB-RO model is used to 0.15.
3. When both temporal and spatial variability are ignored (SU-C model), the simulated monthly AET overestimates the observations with biases of the order of 40%, compared with biases of only 2% when the SV-EB-RO model is used. The irrigation time series at the HRU scale are too smooth and do not match typical farmer irrigation practices, which are known to be event-based. Moreover, the higher availability of water as a consequence of continuous irrigation events increase the modeled AET well above the observed AET.
4. Uncertainty in irrigation inputs can contribute substantially to total uncertainty in the hydrological simulations. For the case study considered here, irrigation schedule uncertainty from the SV-EB-RO model contributes as much as 40% of total simulation uncertainty in the streamflow at the subcatchment scale. At the larger catchment scale, this contribution reduces to around 20%. The reduction in the contribution of irrigation uncertainty at the catchment versus subcatchment scales is likely due to tighter constraints on catchment irrigation through observations, impacts of spatial averaging over the large catchment area, and differences in irrigated land. In other catchments, the importance of irrigation schedule uncertainty will depend on the objectives of the modeling, and the extent of irrigation.

In terms of practical advances, the SV-EB-RO irrigation schedule model proposed in this work will be of value to hydrologists and agriculturalists, including the SWAT community, who use irrigation schedule models to provide inputs into distributed hydrological models and decision-support systems. More generally, this study highlights the importance of representing the spatiotemporal variability of inputs for hydrological models, the use of stochastic models to reflect spatiotemporal uncertainty in simulations of key hydrological quantities, and the use of multivariate environmental data (in this case, streamflow and actual evapotranspiration) to evaluate and refine model assumptions.

Appendix A: Irrigation Schedule Model Algorithms

A1 Spatially Uniform Continuous (SU-C) Irrigation

Irrigation schedule model SU-C (e.g., Chiew & McMahon, 1990) is described by the following algorithm.

A1.1 Inputs

1. Observed catchment irrigation volume time series $I^{cat}_{1:N_t}$.
2. Area of HRUs $A_{1:N_{HRU}}$.
3. Irrigation season data for HRUs, expressed as a time series of Boolean values $s_{1:N_{HRU},1:N_t}$, based on different crop types. Specifically, $s_{h,t} = 1$ indicates that HRU h is "irrigable" (i.e., can potentially be irrigated) at time t. Note that the set of irrigable HRUs defined in section 5.2 can be defined as $h\_irrigable(t) = \{h : s_{h,t} = 1\}$, i.e., the set of HRUs where the indicator flag $s_{h,t} = 1$.

A1.2 Outputs

Simulated irrigation depth $I^{sim}_{1:N_{HRU},1:N_t}$.

A1.3 Procedure

For $h = 1$ to N_{HRU}

For $t = 1$ to N_t

1. Calculate the irrigation depth applied to HRU h for time step t as

$$i_{h,t}^{sim} = I_t^{cat} s_{h,t} / \sum_{n=1}^{N_{HRU}} (A_n s_{n,t})$$

End For t

End For h

A2 Spatially Uniform Event-Based (SU-EB) Irrigation

Irrigation schedule model SU-EB (Githui et al., 2012) is described by the following algorithm.

A2.1 Inputs

1. Observed catchment irrigation volume time series $I_{1:N_t}^{cat}$.
2. Nominal irrigation depth for individual HRUs $r_{1:N_{HRU},1:N_t}$. Note that in this study, r is assumed to be constant across all HRUs and times (see section 3.2.1); however, in practice the nominal irrigation depth r could vary with crop type and time of year.
3. Area of HRUs $A_{1:N_{HRU}}$,
4. Irrigation season data for HRUs, expressed as a time series of Boolean values $s_{1:N_{HRU},1:N_t}$, based on different crop types (e.g., $s_{h,t} = 1$ indicates that HRU h can potentially be irrigated at time t, since the crop type is irrigated in this season).

A2.2 Outputs

Simulated irrigation depth for each HRU and time $i_{1:N_{HRU},1:N_t}^{sim}$.

A2.3 Procedure

For $h = 1$ to N_{HRU}

1. Calculate start date, t_{start}, and end date, t_{end}, of irrigation season for given HRU, based on $s_{h,1:N_t}$
2. Initialize accumulated irrigation depth $i_{h,t_{start}-1}^{accum} = 0$.

   For $t = t_{start}$ to t_{end}

   3. Update accumulated irrigation depth according to

$$i_{h,t}^{accum} = i_{h,t-1}^{accum} + I_t^{cat} r_{h,t} / \sum_{n=1}^{N_{HRU}} (A_n r_{n,t} s_{n,t})$$

   4. If accumulated irrigation depth is greater than the nominal irrigation depth, i.e., $i_{h,t}^{accum} > r_{h,t}$, set $i_{h,t}^{sim} = i_{h,t}^{accum}$ and reset $i_{h,t}^{accum} = 0$.

      Else set simulated irrigation depth $i_{h,t}^{sim} = 0$

   End For t

5. If $i_{h,t_{end}}^{accum} > 0$, set $i_{h,t_{end}}^{sim} = i_{h,t_{end}}^{accum}$

End For h

A3 Spatially Variable Event-Based Irrigation with Random Timing (SV-EB-RT)

Irrigation schedule model SV-EB-RT (Githui et al., 2016) is described by the following algorithm. A difference from Githui et al. (2016) is that we do not calibrate the nominal irrigation depth parameter (referred to as r), instead we keep it at the same fixed value as Githui et al. (2012). This is because calibrating this parameter would require the development of robust calibration techniques that account for the stochastic nature of this model.

A3.1 Inputs

1. Observed catchment irrigation volume time series $I_{1:N_t}^{cat}$.
2. Nominal irrigation depth at individual HRUs $r_{1:N_{HRU},1:N_t}$.
3. Area of HRUs $A_{1:N_{HRU}}$.
4. Irrigation season data for HRUs, expressed as a time series of Boolean values $s_{1:N_{HRU},1:N_t}$, based on different crop types (e.g., $s_{h,t} = 1$ indicates that HRU h can potentially be irrigated at time t, since the crop type is irrigated in this season).

A3.2 Outputs

Simulated irrigation depth for each HRU and time $i^{sim}_{1:N_{HRU},1:N_t}$.

A3.3 Procedure

For $h = 1$ to N_{HRU}

1. Calculate start t_{start} and end t_{end} of irrigation season for given HRU, based on $s_{h,1:N_t}$
2. Initialize accumulated irrigation depth $i^{accum}_{h,t_{start}-1} = 0$.
3. Set irrigation interval number to $\gamma = 1$, and the start of first irrigation interval to $T^{start}_{\gamma} = t_{start}$. An irrigation interval is defined as being a period over which a single irrigation event will occur.

   For $t = t_{start}$ to t_{end}

   4. Update accumulated irrigation depth according to

$$i^{accum}_{h,t} = i^{accum}_{h,t-1} + I_t r_{h,t} / \sum_{n=1}^{N_{HRU}} (A_n r_{n,t} s_{n,t})$$

   5. If accumulated irrigation depth is greater than the nominal irrigation depth, i.e., $i^{accum}_{h,t} > r_{h,t}$, set the end of the irrigation interval to $T^{end}_{\gamma} = t$ and advance to step 6.

      Else, update t and return to step 4.
   6. If $\gamma = 1$, randomly select day τ in the first interval to become the first irrigation event for HRU h, $\tau \sim U[T^{start}_1, T^{end}_1]$, where $U[a, b]$ is the discrete uniform distribution between a and b. The number of days after the start of the interval for which irrigation occurs, $r = \tau - T^{start}_1$, is recorded.

      Else if $\gamma > 1$, the particular day within the irrigation interval for which irrigation occurs is the same as from the first interval, i.e., $\tau = T^{start}_{\gamma} + r$.
   7. Set the simulated irrigation on the selected irrigation day to $i^{sim}_{h,\tau} = i^{accum}_{h,t}$.
   8. Reset $i^{accum}_{h,t} = 0$, update interval number to $\gamma = \gamma + 1$, and set $T^{start}_{\gamma} = t + 1$.

   End For t

9. If $i^{accum}_{h,t_{end}} > 0$, set $\tau = T^{start}_{\gamma} + r$ and $i^{sim}_{h,\tau} = i^{accum}_{h,t_{end}}$.

End For h

A4 Spatially Variable Event-Based Irrigation With Random Ordering (SV-EB-RO)

Irrigation schedule model SV-EB-RO introduced in this work is described by the following algorithm:

A4.1 Inputs

1. Observed catchment irrigation volume time series $I^{cat}_{1:N_t}$.
2. Nominal irrigation depth at individual HRUs $r_{1:N_{HRU},1:N_t}$.
3. Area of HRUs $A_{1:N_{HRU}}$.
4. Irrigation season data for HRUs, expressed as a time series of Boolean values $s_{1:N_{HRU},1:N_t}$, based on different crop types (e.g., $s_{h,t} = 1$ indicates that HRU h can potentially be irrigated at time t, since the crop type is irrigated in this season).

A4.2 Outputs

Simulated irrigation depth for each HRU and time $i^{sim}_{1:N_{HRU},1:N_t}$.

A4.3 Procedure

1. Calculate nominal irrigation volume for each HRU $I^{req}_{1:N_{HRU},1:N_t} = r_{1:N_{HRU},1:N_t} s_{1:N_{HRU},1:N_t} A_{1:N_{HRU}}$, which is the irrigation volume required to irrigate HRUs to the nominal irrigation depth.
2. Randomly shuffle the order of HRUs. We denote the change in order by using a different HRU index, i.e., change from $h = 1 : N_{HRU}$ to $k = 1 : N_{HRU}$.
3. Set the "available" irrigation volume, I^{avail}, which tracks the available irrigation volume that can be used to irrigate the next HRU, to an initial value of $I^{avail} = 0$.
4. Choose the first HRU from the shuffled list, i.e., $k = 1$

   For $t = 1$ to N_t

   5. Update the available irrigation volume to $I^{avail} = I^{avail} + I^{cat}_t$ to add daily catchment irrigation to the remaining available irrigation volume carried over from the previous time step.

6. If available irrigation volume is greater than the nominal irrigation volume for the current HRU, i.e., $I^{avail} \geq I^{req}_{k,t}$, irrigate the current HRU by setting $I^{sim}_{k,t} = I^{req}_{k,t}/A_k$, reduce remaining available irrigation volume $I^{avail} = I^{avail} - I^{req}_{k,t}$, and move onto next HRU by setting $k = k + 1$ and repeat Step 6.

   If there is not enough available irrigation for the next HRU to be irrigated, i.e., $I^{avail} < I^{req}_{k,t}$, carryover the remaining irrigation volume to the next time step t.

End For t

7. Reorder HRUs to $h = 1 : N_{HRU}$. (Since order of HRUs was changed in step 2, we need to change it back to revert to original HRU indices).

Appendix B: Performance Metrics

The Nash-Sutcliffe efficiency (NSE) is a common measure of accuracy of deterministic time series (Nash & Sutcliffe, 1970). For a general set of observed and simulated responses, $(\tilde{\boldsymbol{Y}}, \hat{\boldsymbol{Y}})$, respectively, the NSE is defined as

$$\Phi_{\mathrm{NSE}}[\tilde{\boldsymbol{Y}}, \hat{\boldsymbol{Y}}] = 1 - \frac{\sum_{j=1}^{N_j} (\tilde{Y}_j - \hat{Y}_j)^2}{\sum_{j=1}^{N_j} (\tilde{Y}_j - \mathrm{ave}[\tilde{\boldsymbol{Y}}])^2} \tag{B1}$$

where ave[**z**] denotes the average value of a sample **z** over the considered time period.

A "seasonally adjusted" Nash-Sutcliffe Efficiency, NSE-SA, is better suited to detect errors in short-term fluctuations of variables of interest (Schaefli & Gupta, 2007). The definition of NSE-SA is

$$\Phi_{\mathrm{NSE-SA}}[\tilde{\boldsymbol{Y}}, \hat{\boldsymbol{Y}}] = 1 - \frac{\sum_{j=1}^{N_j} (\tilde{Y}_j - \hat{Y}_j)^2}{\sum_{j=1}^{N_j} (\tilde{Y}_j - \mathrm{ave}_{m(j)}[\tilde{\boldsymbol{Y}}])^2} \tag{B2}$$

where $\mathrm{ave}_m[\tilde{\boldsymbol{Y}}]$ denotes the average observed response value during month m, and $m(j)$ denotes the month when the observed data point indexed j was collected.

The NSE and NSE-SA metrics achieve their maximum value of 1 when the simulations are "perfect". Metric values of 0 indicate the simulations are as accurate as the mean of the observations (calculated over the entire data for the NSE, and based on monthly values for the NSE-SA), and metric values below 0 indicate simulations that are less accurate than the mean of the observations.

The mean bias metric provides a measure of systematic deviation of the simulations from the observations, and is defined as

$$\mathrm{Bias}[\tilde{\boldsymbol{Y}}, \hat{\boldsymbol{Y}}] = \frac{\mathrm{ave}[\hat{\boldsymbol{Y}} - \tilde{\boldsymbol{Y}}]}{\mathrm{ave}[\tilde{\boldsymbol{Y}}]} \tag{B3}$$

Bias values of 0 correspond to unbiased simulations. Positive bias values correspond to simulations that on average over-estimate the observations, and vice versa.

Acknowledgments
This work was supported by the Australian Research Council (ARC) Linkage grant LP100200665 "An integrated modeling framework for the management of irrigated landscapes," and by financial and in-kind contribution from the Department of Economic Development, Jobs, Transport and Resources, Victoria (DEDJTR). The constructive feedback from four anonymous reviewers helped to significantly improve this manuscript, and is gratefully acknowledged. We appreciate the efforts of Benny Selle, for his earlier assistance in organizing the grant application in late 2009, and Kurt Benke, for his insightful suggestions as part of the project's steering committee. We thank the Spatial Sciences Group in DEDJTR, Goulburn-Murray Water, and Jacobs Australia for providing data. The SWAT and PEST input files used in this study are available at https://doi.org/10.6084/m9.figshare.4635121

References

Allen, R. G., Pereira, L. S., Howell, T. A., & Jensen, M. E. (2011). Evapotranspiration information reporting: I. Factors governing measurement accuracy. *Agricultural Water Management*, *98*, 899–920.

Arnold, J. G., Srinivasan, R., Muttiah, R. S., & Williams, J. R. (1998). Large area hydrological modeling and assessment. Part 1: Model Development. *Journal of the American Water Resources Association*, *34*, 73–89.

Baubion, C., DE Marsily, G., Ledoux, E., Li, J., Xin, J., & Huang, S. (2008). Water resources assessment in the Huai River Basin: Hydrological modelling and remote sensing. In *Proceedings Dragon Programme Final Results 2004–2007*, Beijing, China, 21–25 April.

Baumgart, P. D. (2005). Lower Green Bay and Lower Fox Tributary Modeling Report. Paper prepared for Oneida Tribe of Indians of Wisconsin and Green Bay Remedial Action Plan Science and Technical Advisory Committee.

Bergström, S. (1995). The HBV model. In V. P. Singh (ed.), *Computer models of watershed hydrology*. Highlands Ranch, CO: Water Resources Publications.

Beven, K., & Pappenberger, F. (2003). Discussion of 'Towards the hydraulic of the hydroinformatics era'. *Journal of Hydraulic Research*, *41*, 331–336.

Brauer, D., & Gitz, D. (2012). Effects of changes in irrigation and land use on streamflow in the Revuelto Creek Watershed, a Tributary of the Canadian River in New Mexico, USA. *Open Hydrology Journal*, *6*, 88–96.

Cau, P., & Paniconi, C. (2007). Assessment of alternative land management practices using hydrological simulation and a decision support tool: Arborea agricultural region, Sardinia. *Hydrology and Earth System Sciences*, *11*, 1811–1823.

Cheema, M. J. M., Immerzeel, W. W., & Bastiaanssen, W. G. M. (2014). Spatial quantification of groundwater abstraction in the irrigated Indus Basin. *Ground Water*, *52*, 25–36.

Chen, Y., Marek, G. W., Marek, T. H., Brauer, D. K., & Srinivasan, R. (2018). Improving SWAT auto-irrigation functions for simulating agricultural irrigation management using long-term lysimeter field data. *Environmental Modelling & Software*, *99*, 25–38.

Chiew, F. H. S., & Mcmahon, T. A. (1990). Estimating groundwater recharge using a surface watershed modelling approach. *Journal of Hydrology*, *114*, 285–304.

Clark, M. P., Kavetski, D., & Fenicia, F. (2011). Pursuing the method of multiple working hypotheses for hydrological modeling. *Water Resources Research*, *47*, W09301. https://doi.org/10.1029/2010WR009827

Connell, L. D., Jayatilaka, C. J., & Nathan, R. (2001). Modeling flow and transport in irrigation catchments. 2: Spatial application of subcatchment model. *Water Resources Research*, *37*, 965–977.

Consortium Land (2018). *Variations in farm size across the Australia Wheatbelt* [Online], Consortium Land, Perth, Australia. http://www.consortiumland.com/investors/variations-in-farm-size-across-the-australian-wheatbelt/, accessed 15 June 2018.

Doherty, J. (2004). *PEST—Model independent parameter estimation* (5th ed.). Brisbane, Qld: Watermark Numerical Computing.

Emam, A. R., Kappas, M., Akhavan, S., Hosseini, S. Z., & Abbaspour, K. C. (2015). Estimation of groundwater recharge and its relation to land degradation: Case study of a semi-arid river basin in Iran. *Environmental Earth Sciences*, *74*, 6791–6803.

Evin, G., Thyer, M., Kavetski, D., McInerney, D., & Kuczera, G. (2014). Comparison of joint versus postprocessor approaches for hydrological uncertainty estimation accounting for error autocorrelation and heteroscedasticity. *Water Resources Research*, *50*, 2350–2375. https://doi.org/10.1002/2013WR014185

Faramarzi, M., Abbaspour, K. C., Schulin, R., & Yang, H. (2009). Modelling blue and green water resources availability in Iran. *Hydrological Processes*, *23*, 486–501.

Faramarzi, M., Yang, H., Schulin, R., & Abbaspour, K. C. (2010). Modeling wheat yield and crop water productivity in Iran: Implications of agricultural water management for wheat production. *Agricultural Water Management*, *97*, 1861–1875.

Gassman, P. W., Reyes, M. R., Green, C. H., & Arnold, J. G. (2007). The soil and water assessment tool: Historical development, applications, and future research directions. *Transactions of the ASABE*, *50*, 1211–1250.

Githui, F., Gitau, W., Mutua, F., & Bauwens, W. (2009). Climate change impact on SWAT simulated streamflow in western Kenya. *International Journal of Climatology*, *29*, 1823–1834.

Githui, F., Selle, B., & Thayalakumaran, T. (2012). Recharge estimation using remotely sensed evapotranspiration in an irrigated catchment in southeast Australia. *Hydrological Processes*, *26*, 1379–1389.

Githui, F., Thayalakumaran, T., & Selle, B. (2016). Estimating irrigation inputs for distributed hydrological modelling: A case study from an irrigated catchment in southeast Australia. *Hydrological Processes*, *30*, 1824–1835.

Gough, B. (2009). *GNU scientific library reference manual*. Bristol, UK: Network Theory Ltd.

Govender, M., & Everson, C. S. (2005). Modelling streamflow from two small South African experimental catchments using the SWAT model. *Hydrological Processes*, *19*, 683–692.

Greenwood, K. L., Lawson, A. R., & Kelly, K. B. (2009). The water balance of irrigated forages in northern Victoria, Australia. *Agricultural Water Management*, *96*, 847–858.

Irrigating Agriculture (2017). *Weekly irrigation requirements* [Online]. ExtensionAUS Irrigating Agriculture, Victoria, Australia. Retrieved from http://extensionaus.com.au/irrigatingag/weekly-irrigation-requirements/, accessed 19 December 2017.

Kandel, D. D., Western, A. W., & Grayson, R. B. (2005). Scaling from process timescales to daily steps: A distribution function approach. *Water Resources Research*, *41*, W02003. https://doi.org/10.1029/2004WR003380

Kannan, N., Jeong, J., & Srinivasan, R. (2011). Hydrologic modeling of a canal-irrigated agricultural watershed with irrigation best management practices: Case study. *Journal of Hydrologic Engineering*, *16*, 746–757.

Kavetski, D., & Clark, M. P. (2010). Ancient numerical daemons of conceptual hydrological modeling. Part 2: Impact of time stepping scheme on model analysis and prediction. *Water Resources Research*, *46*, W10511. https://doi.org/10.1029/2009WR008896

Kavetski, D., Kuczera, G., & Franks, S. W. (2006). Bayesian analysis of input uncertainty in hydrological modeling: 1. Theory. *Water Resources Research*, *42*, W03408. https://doi.org/10.1029/2005WR004368

Kavetski, D., Kuczera, G., Thyer, M., & Renard, B. (2007). Multistart Newton-type optimisation methods for the calibration of conceptual hydrological models. In Oxley L. and Kulasiri D. (eds) *MODSIM 2007 international congress on modelling and simulation* (pp. 2513–2519), Modelling and Simulation Society of Australia and New Zealand, Christchurch, New Zealand.

Lawson, A., & Hildebrand, K. (2003). *Renovating irrigated perennial pastures: A handbook for Northern Victoria*. Melbourne, Vic: Department of Primary Industries.

Leib, B. G., Hattendorf, M., Elliott, T., & Matthews, G. (2002). Adoption and adaptation of scientific irrigation scheduling: Trends from Washington, USA as of 1998. *Agricultural Water Management*, *55*, 105–120.

Li, X., Yang, X., Gao, Q., Li, Y., & Dong, S. (2009). Integrative assessment of hydrological, ecological, and economic systems for water resources management at river basin scale. *Frontiers of Earth Science in China*, *3*, 198–207.

Maier, N., & Dietrich, J. (2016). Using SWAT for strategic planning of basin scale irrigation control policies: A case study from a humid region in Northern Germany. *Water Resources Management*, *30*(9), 3285–3298.

Marillier, B., Hall, J., & Shakya, D. (2009). *Water-balance modelling of the Leschenault catchment* (Water Sci. Tech. Ser. WST 10). Perth, WA: Department of Water.

McInerney, D., Thyer, M., Kavetski, D., Lerat, J., & Kuczera, G. (2017). Improving probabilistic prediction of daily streamflow by identifying Pareto optimal approaches for modeling heteroscedastic residual errors. *Water Resources Research*, *53*, 2199–2239. https://doi.org/10.1002/2016WR019168

MDBA (2017). *Hydrological modelling using Source* [Online]. Retrieved from https://www.mdba.gov.au/managing-water/hydrological-modelling/hydrological-modelling-using-source Murray Darling Basin Authority, ACT, Australia. Accessed 18 September 2017.

Montagu, K., & Stirzaker, R. (2008). Why do two-thirds of Australian irrigators use no objective irrigation scheduling methods? *WIT Transactions on Ecology and the Environment*, *112*, 95–103.
Nash, J. E., & Sutcliffe, J. V. (1970). River flow forecasting through conceptual models. 1: A discussion of principles. *Journal of Hydrology*, *10*, 257–274.
Neitsch, S., Arnold, J., Kiniry, J., & Williams, J. (2011). *Soil and water assessment tool*. Theoretical Documentation, Version 2009. Temple, TX: Grassland, Soil and Water Research Laboratory Agricultural Research Service, Blackland Research Center, Texas Agricultural Experiment Station.
Ohio EPA (2008). *Total maximum daily loads for the Black River watershed*. Columbus, OH: Division of Surface Water.
Perrin, C., Michel, C., & Andreassian, V. (2003). Improvement of a parsimonious model for streamflow simulation. *Journal of Hydrology*, *279*, 275–289. https://doi.org/10.1016/S0022-1694(03)00225-7
Rahbeh, M., Chanasyk, D., & Miller, J. (2013). Modelling the effect of irrigation on the hydrological output from a small prairie watershed. *Canadian Water Resources Journal*, *38*, 280–295.
Renard, B., Kavetski, D., Leblois, E., Thyer, M., Kuczera, G., & Franks, S. W. (2011). Toward a reliable decomposition of predictive uncertainty in hydrological modeling: Characterizing rainfall errors using conditional simulation. *Water Resources Research*, *47*, W11516. https://doi.org/10.1029/2011WR010643
Sargeant, I. J., Newell, J., & Walbran, W. (1978). *Soils and land use in the Torrumbarry irrigation district*. Melbourne, Vic: Department of Agriculture.
Schaefli, B., & Gupta, H. V. (2007). Do Nash values have value?. *Hydrological Processes*, *21*, 2075– 2080.
Selle, B., Thayalakumaran, T., & Morris, M. (2010). Understanding salt mobilization from an irrigated catchment in south-eastern Australia. *Hydrological Processes*, *24*, 3307–3321.
Sinclair Knight Merz (2005). *Rolling five year review: Statistical analysis of Barr Creek flow and salt load (advanced)*. Tatura, Vic: Goulburn Murray Water.
Skahill, B. E., & Doherty, J. (2006). Efficient accommodation of local minima in watershed model calibration. *Journal of Hydrology*, *329*, 122–139.
SKM (2007). *Smarter management of Barr Creek diversions, Victoria, Barr Creek catchment survey*. Australia: Sinclair Knight Merz.
Smith Murphy, M. (2010). *Application of the Soil and Water Assessment Tool* (*SWAT) to the Willow River Watershed* (Masters). St. Croix County, WI: University of Minnesota.
Sun, C., & Ren, L. (2013). Assessment of surface water resources and evapotranspiration in the Haihe River basin of China using SWAT model. *Hydrological Processes*, *27*, 1200–1222.
Sun, C., & Ren, L. (2014). Assessing crop yield and crop water productivity and optimizing irrigation scheduling of winter wheat and summer maize in the Haihe plain using SWAT model. *Hydrological Processes*, *28*, 2478–2498.
Thyer, M., Renard, B., Kavetski, D., Kuczera, G., Franks, S., & Srikanthan, S. (2009). Critical evaluation of parameter consistency and predictive uncertainty in hydrological modelling: A case study using Bayesian total error analysis. *Water Resources Research*, *45*, W00B14. https://doi.org/10.1029/2008WR006825
Tuteja, N. K., Shin, D., Laugesen, R., Khan, U., Shao, Q., Wang, E., et al. (2012). *Experimental evaluation of the dynamic seasonal streamflow forecasting approach*. Melbourne, Vic: Bureau of Meteorology.
Victorian Resources Online (2017). *How much water does perennial pasture need?* [Online]. Agriculture Victoria, Victoria, Australia. Retrieved from http://vro.agriculture.vic.gov.au/dpi/vro/vrosite.nsf/pages/lwm_farmwater_efficient_irrigation_2.3.1, accessed 29 January 2018.
Wang, X., & Melessa, A. M. (2005). Evaluation of the SWAT model's snowmelt hydrology in a northwestern Minnesota watershed *Transactions of the ASAE*, *48*, 1359–1376.
Zeng, R., & Cai, X. (2014). Analyzing streamflow changes: Irrigation-enhanced interaction between aquifer and streamflow in the Republican River basin. *Hydrology and Earth System Sciences*, *18*, 493–502.